Energy Dependent Relative Cross Sections in Carbon $1s$ Photoionization. Separation of Direct Shake and Inelastic Scattering Effects in Single Molecules

Oksana Travnikova,[*,†,‡] Minna Patanen,[¶] Johan Söderström,[§] Andreas Lindblad,[§] Joshua J. Kas,[‖] Fernando D. Vila,[‖] Denis Céolin,[‡] Tatiana Marchenko,[†,‡] Gildas Goldsztejn,[†] Renaud Guillemin,[†,‡] Loïc Journel,[†,‡] Thomas X. Carroll,[⊥] Knut J. Børve,[#] Piero Decleva,[@] John J. Rehr,[‖] Nils Mårtensson,[§] Marc Simon,[†,‡] Svante Svensson,[§] and Leif J. Sæthre[*,#]

LCPMR, CNRS, Sorbonne Université, UMR7614, Paris, France, Synchrotron Soleil, L'Orme des Merisiers, Saint-Aubin, F-91192 Gif-sur-Yvette Cedex, France, Nano and Molecular Systems Research Unit, Faculty of Science, P.O.Box 3000, 90014 University of Oulu, Finland, Department of Physics and Astronomy, Uppsala University, P.O. Box 516, 75120 Uppsala, Sweden, Department of Physics, Box 351560, University of Washington, Seattle, Washington 98195-1560, USA, Division of Natural Sciences, Keuka College, Keuka Park, New York 14478, USA, Department of Chemistry, University of Bergen, Allégaten 41, NO-5007 Bergen, Norway, and Dipartimento di Scienze Chimiche e Farmaceutiche, Universitá di Trieste and IOM-CNR, 34127 Trieste, Italy

E-mail: Oksana.Travnikova@upmc.fr; Leif.Saethre@uib.no

Abstract

We demonstrate that the possibility of monitoring relative photoionization cross sections over a large photon energy range allows studying and disentangling shake processes and intramolecular inelastic scattering effects. In this gas phase study, relative intensities of the C 1*s* photoelectron lines from chemically inequivalent carbon atoms in the same molecule have been measured as function of incident photon energy in the range of 300 – 6000 eV. We present relative cross sections for the chemically shifted C 1*s* lines in the photoelectron spectra of ethyl trifluoroacetate (the "ESCA" molecule). The results are compared to those of methyl trifluoroacetate and S-ethyl trifluorothioaceetate, as well as a series of chloro-substituted ethanes and 2-butyne. In the soft X-ray energy range, the cross sections show EXAFS-type of wiggles, as was previously observed for a series of chloroethanes. The oscillations are damped in the hard X-ray energy range, but deviations of cross-section ratios from stoichiometry persist even at high energies. The current findings are supported by theoretical calculations based on a multiple scattering model. The use of soft and tender x-rays provides a more complete picture of the dominant processes accompanying photoionization. Such processes reduce the main photoelectron line intensities by 20-60%. Using both energy ranges enabled to discern the process of intramolecular inelastic scattering of the outgoing electron, whose significance is otherwise difficult to assess for isolated molecules. This effect relates to the notion of the Inelastic Mean Free Path (IMFP) commonly used in photoemission studies of clusters and condensed matter.

*To whom correspondence should be addressed

†LCPMR, CNRS, Sorbonne Université, UMR7614, Paris, France

‡Synchrotron Soleil, L'Orme des Merisiers, Saint-Aubin, F-91192 Gif-sur-Yvette Cedex, France

¶Nano and Molecular Systems Research Unit, Faculty of Science, P.O.Box 3000, 90014 University of Oulu, Finland

§Department of Physics and Astronomy, Uppsala University, P.O. Box 516, 75120 Uppsala, Sweden

‖Department of Physics, Box 351560, University of Washington, Seattle, Washington 98195-1560, USA

⊥Division of Natural Sciences, Keuka College, Keuka Park, New York 14478, USA

#Department of Chemistry, University of Bergen, Allégaten 41, NO-5007 Bergen, Norway

@Dipartimento di Scienze Chimiche e Farmaceutiche, Universitá di Trieste and IOM-CNR, 34127 Trieste, Italy

Introduction

Cross sections for core photoionization of free molecules, liquids and solids have been studied for decades. Already in the very first monograph on ESCA (Electron Spectroscopy for Chemical Analysis) from 1967 it was observed that the intensities in the electron spectra of core levels corresponded to the stoichiometric ratios.[1,2] This observation has formed the basis for using electron spectroscopy as a quantitative tool, i.e. for obtaining stoichiometric information of inequivalent species in a sample. Later investigations have shown that this principle has to be modified e.g. due to the influence of site-specific probabilities of shake processes.[3,4] The present work is part of an ongoing effort to understand the limitations to the quantitative interpretation of relative core-line intensities.

In the case of condensed matter samples, one has long been aware of severe problems in relating stoichiometry to observed relative photoelectron intensities. The short electron mean free path (at kinetic energies commonly used in soft X-ray Photoelectron Spectroscopy (XPS)) makes the core electron signal (per atom) from atoms in the bulk less intense than the signal from those at the surface. This has been extensively exploited for depth profiling where the surface/bulk sensitivity is changed by varying either the energy or the angle of the incident photon beam. A careful depth analysis typically requires a priori knowledge of inelastic mean free paths (IMFP) and photoionisation cross-sections. IMFP often rely on semi empirical formulae,[5–8] and very often the cross sections quoted in literature are taken from a theoretical work of Yeh and Lindau,[9] a study that is based on purely atomic calculations. However, the relevance for molecules has not been tested enough experimentally.

In condensed matter samples there are also cross section effects of the same type as seen in EXAFS (Extended X-ray Absorption Fine Structure).[10–13] Furthermore, there are also photoelectron diffraction effects which introduce angle- and energy dependent intensity variations that may be very pronounced for solids and surfaces.[11,14] However, it is very difficult to disentangle these effects and not so much progress has been reported. One important experimental issue is that in order to determine the photoionization cross section, the angle-differential cross section has to be

integrated over the full sphere so as to average out photoelectron diffraction effects. This is, of course, impossible in the case of a surface, and therefore Photoelectron Extended X-ray Absorption Fine Structure (PEXAFS) has not been widely used.[12,13] However, relative PEXAFS signals from chemically shifted photoelectron lines of different coordination states or different spin-orbit components allow one to single out the scattering effects as has been demonstrated for surfaces[15] and clusters.[16,17]

It is well known that a large part of the total cross section goes to shake-satellite processes (shake-up and shake-off) caused by the creation of the core hole. The general theory for shake processes in molecules was obtained already in the 1970s.[18] In Ref.[19] a distinction is made between direct and conjugate transitions. At high kinetic energies of the photoelectrons, the direct transitions dominate. The conjugate shake is of minor importance already 100 eV above the threshold.[20]

For gas phase samples also satellites due to inelastic scattering of the photoelectrons on the way to the detector must be considered. However, these processes are easy to detect since the intensity varies with the square of the pressure. At sufficiently low pressure we show that inelastic scattering within the ionized molecule itself also gives a significant contribution to the cross section already for small molecules.

The widely-used theoretical framework for these processes has its basis in solid state core-level spectroscopy, and thus the nomenclature stems from there as well. The *intrinsic* effects relate to the change in the electronic structure caused by photoionization and the consequent change of the molecular electrostatic potential. Different shake processes (direct and conjugate) are referred to as intrinsic effects. However, in the present work conjugate shake is not taken into account in theoretical calculations because of the rather small photon energy range of its importance and demanding computational requirements for its description.

The *extrinsic* effects describe interactions of the outgoing electron with other electrons in the system as it travels through the surrounding molecular media, i.e. electron transport.[21] In their essence, intrinsic and extrinsic effects are the same for isolated molecules and solids (a single molecule can be viewed as an ensemble of atoms). In our molecular case, extrinsic effects can be

only intramolecular. In the following we use *intramolecular inelastic scattering (IIS)* to refer to extrinsic effects in individual molecules. The present work allows isolating and describing inelastic scattering effects occurring within a single molecule in the vicinity of the ionization site, which are also present in solids and constitute a significant part of all inelastic scattering effects occurring in solids.

We have previously demonstrated that gas-phase core-electron photoemission[22,23] offers an efficient approach to study the site dependence of cross sections, which is inaccessible from commonly used total-yield methods.[24] In the gas phase, the combined effect of low sample density and random orientation of molecules effectively smears out all effects of extramolecular photoelectron diffraction and therefore cross-section effects can be accessed. Moreover, choosing a model system with atoms of the same element but in different chemical environments facilitates the use of an internal calibration of intensities, by considering the *relative* dependence on the energy of the photoionization cross section. In an earlier report we presented the relative energy dependence of cross sections for mono-, di- and trichlorinated ethane in a series where the CH_3 end of the molecules was a common motif, CH_3–CH_xCl_{3-x}, $x = 0, 1, 2$. The result showed an "EXAFS"-type of oscillatory behavior (see below) of the relative C 1*s* cross sections in a wide energy range from the threshold to a photoelectron kinetic energy of 500 eV.[22] The amplitude of the oscillations increases with the degree of chlorination, and the oscillatory behavior was rationalized in terms of backscattering of the outgoing photoelectron wave on chlorines, which were perceived as strong scatterers (compared to hydrogen) on account of its electron-rich valence shell. These oscillations persist for dissolved species, implying that the effect has to be considered when performing depth-profiling experiments of solutions and condensed matter by varying the photon energy, especially relatively close to ionization threshold (<200 eV kinetic energy).[25]

Intensity oscillation in C 1*s* cross sections has also been studied for 2-butyne (CH_3-C≡C-CH_3), for photon energies ranging from threshold to about 150 eV above threshold.[23] The intensity ratio between the triply bonded carbons and the methyl carbons ($C_{C\equiv C}$/C_{CH_3}) varies with the photon energy in a similar manner to what is observed for the chloroethanes. This was surprising on ac-

count of 2-butyne contains no *a priori* strong scattering centers but rather two carbon atoms where the number of neighboring non-hydrogen atoms is different. This example shows that intensity oscillations and nonstoichiometric ratios can be expected also as a result of differences in chemical bonding owing to different electron densities in the vicinity of the ionization site.

Note that, oscillations in photoionization cross-sections can also be observed in molecules with equivalent atomic sites. In such cases the two outgoing electron waves emitted by equivalent centers can interfere in a way similar to the celebrated Young's double-slit experiment (e.g. N_2,[26,27] C_2H_2[28–31]). The interference patterns, i.e. the oscillation periods for inner- or valence-shell photoionization, are dependent on the interatomic distances, which may open an approach to structure determination.[32] The photoelectron diffraction principle can be also used to derive the molecular geometry for isolated small molecules by analyzing the ratios of vibrationally resolved photoionization cross sections.[33–35]

In the present study we focus on the C 1*s* spectrum of ethyl trifluoroacetate, CH_3CH_2O–(C=O)–CF_3 (the so-called *"ESCA"* molecule) as well as two substitutionally related molecules. The ESCA molecule is chosen on account of its C 1*s* spectrum being dominated by large chemical shifts between the four carbon atoms,[36] which facilitates the present analysis. Contrary to Ref.,[22] which explored the impact on relative C 1*s* cross sections from changing the number of a substituent (chlorine) attached to a single carbon, the ESCA molecule is well suited for comparing the effect of the local chemical environment on relative cross sections. This molecule offers four sites for C 1*s* ionization, covalently bonded to different 2^{nd}-row atoms C, O and F. The two substituted compounds alluded to above, are the methyl and thio analogues of the ESCA molecule, conventionally named methyl trifluoroacetate [CH_3O–(C=O)–CF_3, or M-ESCA for short] and S-ethyl trifluorothioacetate [CH_3CH_2S–(C=O)–CF_3, or S-ESCA for short], respectively. The C 1*s* spectra of these molecules are used to probe the effect of different substituents (methoxy vs ethoxy, thioether vs ether) on the relative intensities of photoemission lines.

Unprecedented, we have investigated the energy dependence of relative cross sections from soft X-rays, across the *tender* interval (2-4 keV) and touching upon the hard X-ray regime (>5

keV). Following the recipe used for the soft X-ray regime, we first extended the study reported in Ref.[22] of the three chloroethanes to photon energies ranging from about 2 to 6 keV. With the chloroethanes forming a frame of reference, the ESCA molecule as well as 2-butyne[23] are explored in a similar manner. In addition to exemplifying how variations in relative cross sections are reduced with increasing photoelectron energy, the observations are applied to a discussion of the various mechanisms that may give rise to departure from stoichiometric ratios.

Furthermore, comparing low- and high-energy data of the main photoemission lines, we demonstrate a way to access the relative strengths of different inelastic multielectron effects, such as shake processes and IIS, which accompany photoionization in addition to photoelectron elastic scattering. Their relative strengths can be estimated from the experimental data due to their different energy dependence. Though the suggested experimental method does not allow extraction of absolute magnitudes of elastic scattering, shake processes and IIS, it can serve as a tool for prediction of influences of different molecular environments on these effects. Experimental data is compared with theoretical calculations that take into account both multiple (elastic) scattering as well as inelastic intrinsic (direct shake) and extrinsic (IIS) effects, which reduce the cross section of the direct, usually dominant, photoemission channel.

Experimental Details

The experiments were performed at the PLEIADES[37,38] and GALAXIES beamlines[39,40] at the French national synchrotron SOLEIL, and at the I411 beamline[41] at the Swedish national synchrotron MAX II. The low-energy data was measured at PLEIADES and I411, whereas the high-energy data was collected at the GALAXIES beamline.

The low-energy measurements at the PLEIADES beamline were performed using a wide-angle lens VG-Scienta R4000 electron spectrometer installed at a fixed position, with the electron detection axis perpendicular to the storage-ring plane. The polarization vector of the X-ray light has been set at the so-called magic angle of 54.7° with respect to the electron detection axis. The

degree of linear polarization of the photon beam was characterized before the experiment[37] and found to be better than 98%. However, since the experiments were performed at the magic angle the eventual influence of the polarization can be neglected. Data was measured at photon energies of 305 eV, in steps of 20 eV between 310 and 600 eV, and at 650 and 700 eV. Pass energies of 10, 20, 50 and 100 eV were used in order to strike a useful balance between intensity and resolution as well as to operate the analyser within the limits of the kinetic energies usable for each pass energy. In order to verify the consistency of the results, at least two spectra were recorded with the same photon energy but different pass energies whenever the pass energy was changed.

The low-energy measurements at the I411 beamline at MAX II were performed using the Scienta R4000 analyzer, installed perpendicular to the beam direction and at the magic angle to the polarization direction. In general, data was collected at photon energies from 305 eV to 450 eV, in steps of 5 eV for the lower part of the energy range and in steps of 10 eV at higher energies. In addition, more measurements were included in areas of rapid intensity variation. Measurements at selected energies were repeated to monitor the reproducibility of the obtained values. Absolute calibration of the binding energy scale was accomplished from measurements of the sample mixed with carbon dioxide, using the adiabatic carbon $1s$ energy of CO_2.[42] The CO_2 spectrum also provided information of the total instrument resolution as found from the Gaussian component of the full width at half-maximum (FWHM). Monochromator and spectrometer settings were chosen to provide a reasonable compromise between intensity and resolution. In the present case the estimated experimental resolutions were of about 80 meV at 340 eV and 140 meV at 490 eV. For the ESCA family members rather wide scans were necessary, but since the inherent line widths are broad the results are not largely dependent on instrumental resolution. It should also be noted that the results presented here for the ESCA molecule represent experiments at two different synchrotrons using two different experimental setups at two different times – hence the consistency of the results can be judged from the spread in the data, which was used to estimate the error bars.

The high-energy measurements achieved at the GALAXIES beamline of the synchrotron SOLEIL use a wide-angle VG-Scienta EW4000 spectrometer installed at the hard x-ray photoelectron spec-

troscopy (HAXPES) end-station.[39] In brief, the beamline delivers linearly polarized light, which is monochromatized by a Si(111) double crystal and focused by a toroidal mirror. The photon bandwidth is ∼250 meV around 3 keV and ∼1 eV around 6 keV. The spectrometer is installed parallel to the light polarization vector. The spectrometer pass energy was set to 100 eV for the measurements performed at photon energies of 2300 and 3800 eV, and 200 eV for the photon energies above 4000 eV to obtain a better signal-to-noise ratio. Pertaining to the high-energy measurements, a statistical analysis was used to derive relative uncertainties for the branching ratios. The thus estimated uncertainties are rather low, between 0.5–1.5%, and most likely underestimated.

Ethyl trifluoroacetate (99%), methyl trifluoroacetate (99%), and *S*-ethyl trifluorothioacetate (≥98%), as well as chloroethane (99.7%), 1,1-dichloroethane (99,998%), 1,1,1-trichloroethane (99.998%) and 2-butyne (99%) were all obtained from Sigma-Aldrich. Except for gaseous chloroethane all samples are liquids at room temperature, and dissolved air and possible volatile impurities were removed by several freeze-pump-thaw cycles. The samples were introduced into a differentially pumped gas cell via a gas inlet system. The pressure of the sample in the vacuum chamber was kept constant around 7×10^{-6} mbar for the measurements at the PLEIADES beamline, $\sim 5-6 \times 10^{-6}$ mbar at the GALAXIES beamline, and at about 8×10^{-6} mbar for the measurements at the I411 beamline.

Data treatment

C 1*s* photoelectron lines were fitted using Igor Pro software by WaveMetrics, Inc. and the SPANCF curve fitting macro package by E. Kukk.[43,44] Two approaches were used: a so-called "best-fit model" and theoretical Franck-Condon profiles.

In the "best-fit" approach, also used in Ref.,[22] each carbon photoelectron line is fitted using two harmonically spaced vibrational progressions. It is important to point out that this is not a full vibrational analysis; instead the fits are performed on a "best fit" basis. Such a simple approach is possible to use since we make use of only the total peak intensities in our analysis and no specific information regarding individual vibrational components.

For the fits using theoretical profiles, Franck-Condon factors were calculated as described previously for the ESCA molecule,[36] the chloroethanes,[45] and 2-butyne.[46] Post-collisional interaction (PCI) line shapes[47] were adopted in the fitting of the low energy data close to the ionization threshold. The Gaussian width accounting for the instrumental and translational Doppler broadening was set to the same value for all peaks for a given photon energy.

In the case of chlorinated ethanes and the ESCA-molecule, both the "best-fit model" and Franck-Condon profiles were used to fit the experimental data separately for comparison of the two methods. The results obtained by the two methods were essentially the same. However, the "best-fit model" describes less accurately overlapping structures. Therefore, for a more reliable comparison of the ratios for the ESCA family members (ESCA, S-ESCA, M-ESCA) Franck-Condon profiles were used to extract the peak areas.

All high-energy data was fitted using calculated vibrational profiles to avoid ambiguity caused by a non-negligible overlap of the C 1s photoelectron lines due to lower resolution in this energy range (2.3-6 keV) and larger Doppler broadening of the corresponding high-kinetic energy photoelectron lines.

In the case of the chloroethanes we observed a strong background from Cl 2s shake contributions. Subtraction of this was made using a model taken from a Cl 1s shake spectrum. For further details see Supplementary Material.

In contrast to measurements at PLEIADES and I411, at GALAXIES the angle θ between the detected photoelectrons and light polarization vector is fixed to 0°. If the photoionization angular distribution parameters (β) of the two inequivalent C atoms differ, their intensity ratio is dependent on θ and therefore different between the measurement performed at the magic angle ($\theta = 54.7°$) and the measurement with the photoelectron vector parallel to the light polarization axis ($\theta = 0°$). In our previous work,[45] we observed that the β parameter for C 1s photoionization of the chlorinated C-atom (β_{CCl_x}) deviates more from that of the methyl carbon (β_{CH_3}) the more chlorinated the molecule is. β_{CH_3} recorded for photoionization energies up to about 300 eV above the C 1s threshold, approaches the value 2, while β_{CCl_x} does not seem to reach this value. Using the well-known

equation[48] (1) of differential photoionization cross-section $\delta\sigma/\delta\Omega$ in dipole approximation for linearly polarized light with degree of polarization p

$$\frac{\delta\sigma}{\delta\Omega} = \frac{\sigma_{tot}}{4\pi}\left[1+\frac{\beta}{4}(3p\cos 2\theta + 1)\right] \tag{1}$$

we can express the photoionization cross section at 0° as eq. 2 (assuming $p = 1$):

$$I^{0^\circ} = I^{54.7^\circ}(1+\beta) \tag{2}$$

Thus, the ratios recorded at 0° can be corrected to correspond the magic angle data by multiplying with a factor taking into account the different β parameters using the following expression:

$$\frac{I^{54.7^\circ}(C_{CCl_x})}{I^{54.7^\circ}(C_{CH_3})} = \frac{I^{0^\circ}(C_{CCl_x})\left[1+\beta_{CH_3}\right]}{I^{0^\circ}(C_{CH_3})\left[1+\beta_{CCl_x}\right]} \tag{3}$$

The theoretical β parameters for chloroethanes and the ESCA molecule are available in the literature only for relatively low kinetic energies up to 300 and 100 eV, respectively, where asymptotic limits are not reached yet.[45,49] To estimate the correction factor at high energies, we have calculated β parameters up to electron kinetic energies 570 and 530 eV for chloroethanes and the ESCA molecule, respectively. The details of the calculations are to be discussed below. The correction in the order of $\leq 2\%$ resulted in slightly higher ratios. The largest correction factors are for the CCl_3/CH_3 ratio (1.4%) in 1,1,1-trichloroethane and CF_3/CH_3 (2.1%) and C=O/CH_3 (1.6%) ratios in ESCA . The correction factor for 2-butyne was estimated to be less than 1% on the basis of β parameters up to 500 eV kinetic energy.

Ab initio calculations of asymmetry parameters become very demanding with increasing electron kinetic energy and loss of molecular symmetry. To verify the trends in β-values for higher photoelectron kinetic energies, we have calculated β up to kinetic energy of about 1300 eV for 1,1,1-trichloroethane only. After about 700 eV, β parameters for C_{CCl_3} and C_{CH_3} carbon atoms go smoothly towards the asymptotic limit close to 2 and the differences between the two chemically

inequivalent atoms gradually decrease. The correction factor for CCl_3/CH_3 at 1300 eV is below 1%. Therefore, at higher kinetic energies (>2 keV) the correction for all the measured molecules is expected to be within our experimental uncertainties.

Accordingly, the different acceptance angles of the spectrometers used were estimated to introduce deviation in ratios on the order of less than 0.1%, which is not observable in our measurements.

Calculations

Di Tommaso and Decleva[49] have calculated both the C 1*s* cross section σ and asymmetry parameter β of the ESCA molecule and observe large variations in the cross section ratio near threshold. For practical reasons our experimental data do not extend as close to the ionization thresholds as in Ref.[49] but has a lowest photon energy of 305 eV. However, our data extends to several keV above the thresholds.

To complete the theoretical predictions we made use of the theoretical framework presented in Ref.[22] We computed the 1s X-ray absorption spectra (XAS) for each carbon atom in the molecule using the FEFF9 real-space multiple scattering code.[50,51] We made calculations both for the *anti-anti* and *anti-gauche* conformations, but found that the results were essentially identical. We obtained *ab initio* Debye-Waller factors with an efficient Lanczos algorithm for projected phonon spectra, and dynamical matrices from Gaussian 09 (G09).[52,53] Multiple scattering calculations have proven to be quite accurate from energies roughly 30 eV above ionization threshold, and are limited only to the accuracy of input parameters such as structure and vibrational effects. Typically these calculations yield uncertainties in fine-structure amplitudes of order 10% and periods of order 1%, consistent with the results reported here. Available experimental structures were used[54–60] and their associated Hessians were obtained at the B3LYP/aug-cc-pVTZ level of theory. For the molecules calculated here, this combination of functional and basis set type yields sufficiently accurate structures and vibrational properties.[61]

The intrinsic amplitude reduction factors, corresponding to direct shake processes, have been estimated using the so-called "sudden approximation"[62,63] from S_0^2, the square of the overlap integral between the initial state wave function and the relaxed final-state wavefunction with the active core electron annihilated (see section "Mechanisms for intensity reduction of photoelectron lines" for a description of the sudden approximation). These wave functions were estimated in the Δ SCF approximation using Gaussian,[53] i.e., the ground state wavefunction was computed with the HF method, while the final state one was computed using the CASSCF method with a restricted active space that limits the calculation to a single configuration with the core electron removed.

In order to take IIS effects (i.e. extrinsic effects) into account we used a semi-classical expression for the electron propagator, and a local density approximation for the inelastic mean free path (IMFP), as described in detail by Hedin et al.[64] Before taking the ratios of the calculated cross sections, we calculated the chemical shifts for each transition using Koopmans' theorem and the B3LYP functional, and shifted the XAS appropriately.

Thus, the total theoretical curves are products of three contributions – (1) elastic multiple electron scattering, (2) energy-independent intrinsic amplitude reduction factors, (3) extrinsic amplitude reduction factors, – which were calculated separately and multiplied to give a final result (shown as dotted green curves in Figs. 5 and 6). However, the ratios extracted from the experimental data are typically smaller. We use the average experimental values above 2 keV to fit theoretical curves to experimental ratios. Therefore, the theoretical curves in Fig. 2 and Fig. 6 have been additionally multiplied by a factor of 0.99, 0.96 and 0.99 for the CF_3/CH_3, C=O/CH_3 and the CH_2/CH_3 ratios, respectively. The correction factors used for adjustment of the theoretical curves of chloroethanes in Fig. 5 are 1.00, 0.98 and 0.92 for the CH_2Cl/CH_3, $CHCl_2/CH_3$ and the CCl_3/CH_3 ratios, respectively. At high energies, contributions of energy-dependent processes (IIS, conjugate shakes) to the reduction of the main photoline intensity should be negligible and only direct shake effects are present. In this way the correction factors provide an estimate of the accuracy of the used theoretical approach for the description of the energy-independent part of intrinsic effects. (Note that this adjustment is different from the one in Ref.,[22] where theoretical

curves were adjusted to match the experimental values at 750-800 eV)

Calculations of β parameters were performed using the LCAO B-spline code, as described in Ref.[45] for the CH_3-CCl_3 molecule, and similarly for 2-butyne and the ESCA molecule. Maximum angular momentum quantum number employed is $L_{max} = 40$, which ensured convergence up to a maximum electron kinetic energy of 1300 eV for CH_3-CCl_3, and 500 eV for 2-butyne and the ESCA molecule.

Vibrational transitions accompanying each photoelectron line were calculated within the Franck-Condon approximation for the ESCA, M-ESCA, S-ESCA and the three chloroethane molecules. Details of the calculations for chloroethanes and ESCA molecule can be found in Refs.[36,45] In short, geometries for the ground and ionized states, normal modes, and harmonic frequencies of chloroethanes were calculated at the MP4SDQ level of theory while density functional theory (DFT) with B3LYP functional was employed for ESCA, M-ESCA and S-ESCA. The G09 package of programs were used in both cases.

For the ESCA family members the Franck-Condon analysis was carried out in the linear-coupling approximation. This implies that the initial-state normal modes and the corresponding vibrational frequencies are used also for the ionized states, and that for each ionized state, an effective displacement of the potential minimum relative to that of the ground state is obtained by requiring that the potential model should reproduce the computed final-state gradient in the initial-state geometry.

Mechanisms for intensity reduction of photoelectron lines

It must be emphasized that we report the ratios of areas of the main C 1*s* photolines, thus any relative change that can reduce their intensity is accounted for. In this section we give a brief summary of the shake effects and other possible mechanisms, which might lead to intensity losses of photoelectron lines. To discern between the so-called *intrinsic* and *extrinsic* effects, we can relate the intrinsic ones to the interactions of the passive electrons with the core-hole, while the

extrinsic ones are associated with the dynamic electron interactions between the passive electrons and the escaping photoelectron as it transverses the surrounding system on its way out to the continuum.

It has been known since a long time that the relative intensities of core-photoelectron lines do not correspond exactly to the stoichiometric ratios, even at high excess energies, such as in the case of AlK_α excitation ($h\nu$=1487 eV), see e.g. Ref.[3] The most important reason for this is that shake-up and shake-off processes also contribute to the spectrum. The total shake probability for a specific core ionization site clearly influences the line intensities. The deviation of relative ionization cross-sections from stoichiometric values, normally in the order of about $\leq$10%, has also been pointed out for high excess energy e.g. in Ref.[13] However, in some cases, e.g. for metal complexes[65] and for aromatic donor-acceptor molecules[66] it may be much larger, since the total shake probability is very high in these cases. Interestingly, this relation between stoichiometry and line intensities has not been investigated very systematically and one can easily find examples, notably in applied electron spectroscopy, where a very simple one-to-one correspondence has been more or less tacitly assumed. In order to relate stoichiometric factors and core-electron line intensities one obviously needs to determine the shake probabilities. This is often done experimentally,[67–71] however this task also benefits from theoretical support.[19,72–75]

The influence of the shake processes on the results presented here cannot be addressed without discussion of the two main shake mechanisms: direct shake-up and conjugate shake-up. A compact description of these processes was given by Martin and Shirley for free atoms[72] and Arneberg et al. for molecules.[19] The two mechanisms will be considered below.

According to the sudden approximation,[20,62,63] the sudden change in the molecular potential due to the disappearance of a core electron (core ionization) can 'shake' a valence electron to an unoccupied orbital. This occurs due to the adjustment of passive electrons to screening of a formed electron vacancy, which results in shrinkage of electronic shells in the ionised state. In essence, this process is photon-energy independent – the way the core hole was created does not play a role. The exception is the photon energy range very close to the threshold, when relaxation of electrons

is a dynamic process influenced by a continuously changing interaction with the outgoing slow photoelectron.[76] In direct photoionization, the photon is absorbed by a core electron, which is then emitted to the continuum. The angular momentum of the photon is transferred changing the symmetry of the outgoing electron wave by an odd number, in most likelihood, 1 ($\Delta l \pm 1$). Monopole selection rules then apply for accompanying electronic excitation. For example, direct shake-up states can be created when $1s$ dipole ionization occurs simultaneously with $2s \rightarrow ns$ or $2p \rightarrow np$ monopole shake excitations.

In addition to shake-up, there is shake-off, which is similar to direct shake-up except that now the secondary electron is *shaken off* to the continuum and hence the remaining ion is left doubly charged after photoionization. It is known to be of comparable probability to direct shake-up in rare gases.[77,78] Even if shake processes in atoms have been extensively studied, little is known about how they are affected by the molecular environment, especially at high excess energy.

These effects are accounted for as intrinsic amplitude reduction factors in the present theoretical description. Intensity losses due to direct shake effects were evaluated from the overlap integrals of ground and core-holes states at the HF level (see above). This relatively simple theoretical description of direct shakes is generally reasonable and computationally cost-effective. However, it is incomplete because it does not allow representing the multi-electron excitation effects, which cannot be described within one-particle picture and require consideration of more complex configuration interactions to account for the change in correlation of the many-electron system.[79,80] Further on we will use "multi-electron correlation satellites" to refer to correlation satellites requiring multiple electron excitations.[81] The probability of multi-electron correlation satellites increases with the atomic Z number and becomes important already for atoms possessing $3s$ electron shells (such as S, Cl *etc.*).[82,83]

In contrast, in the case of conjugate shakes, the photon is absorbed by a valence electron inducing its excitation, which is accompanied by shake-off of a core electron due to relaxation of passive electrons. The photon angular momentum is hence exchanged with the excited electron and the symmetry of the outgoing photoelectron wave is preserved ($\Delta l = 0$).[63] For example, a conjugate

$1s^{-1}2s^{-1}np^1$ state can be produced, when $1s$ electron is emitted as an s-wave and simultaneously $2s \rightarrow np$ dipole excitation occurs. The same conjugate $1s^{-1}2s^{-1}np^1$ state can be also represented as a dipole excitation of $1s$ electron to an unoccupied np orbital accompanied by shake-off of a $2s$ electron. Therefore, the conjugate shake-up process is in essence resonance-like[20,63,76,84] and has a pronounced dependence on the ionization energy. The probability for a conjugate shake-up is particularly strong close to the threshold and decreases monotonically with increasing photon energy. At high photon energies it is expected that direct shake-up transitions dominate and that conjugate processes can be neglected for energies over 100 eV above threshold.[63,68,69,85,86] Therefore, when discussing the high-energy results in this paper, conjugate shake-ups can safely be disregarded. In the present theoretical description, conjugate shake processes were not considered. However, it should be mentioned that for low-cross-section photoionization processes, such as double-core-electron photoionization, direct and conjugate shake-up probabilities can be of comparable magnitudes even several keV above threshold.[84,87]

In rare gas and alkali metal atoms, other processes, known as *knock-out*, and its energy dependence have been extensively studied (see e.g.[88–91]). Knock-out can be illustrated as an electron collision process inside the molecule, similar to (e,2e) or electron impact.[92] The selection rules for knock-out satellites are different from direct and conjugate shakes allowing transitions with the change of the angular momentum $\Delta l > 1$. It can be mentioned that knock-out can also lead to the same final states as produced by direct and conjugate shake processes but with considerably lower cross sections. Quantum-chemically knock-out is described as interchannel coupling, when final continuum states are mixed, so that intensity may be transferred from one channel to another. Schneider et al.[93] reported the excess energy dependence of knock-out versus shake-off mechanisms of double ionization in He, showing that the shake-off becomes more important than the knock-out at about 350 eV above the ionization threshold and is twice as important at 1000 eV owing to the rapid decrease of the knock-out probability.

When the kinetic energy of the outgoing photoelectron is high enough, new knock-out and shake channels open: high-kinetic-energy outgoing electrons can induce ionization or excitation

of electrons from core shells, such as neighbour Cl $2p$, $1s$, O $1s$ or C $1s$ shells. This would involve a creation of a two-site double-core-hole states (e.g. C$1s^{-1}$O$1s^{-1}$, C$1s^{-1}$Cl$2p^{-1}$). Noteworthy, the cross sections for double core holes are known to be very small, four to five orders of magnitude weaker than the corresponding single-core-hole ionization,[94–96] which is far below the error bars of our measurements.

In the theoretical framework used here, *intramolecular inelastic scattering* (IIS) mechanisms reducing the intensity of the main C$1s$ lines due to interactions of the outgoing photoelectron as it propagates through the molecule, are evaluated as extrinsic effects. IIS, including knock-out, is photon energy dependent. Electrons with low kinetic energy have more time for interactions and energy exchange, while fast electrons leave the molecule so quickly that there is no time to transfer energy to other electrons in the system. Moreover, the larger number of many-electron substituents close to the ionization site would lead to higher probability of inelastic scattering and, more importantly, intensity losses of the main photoionization lines.

Extrinsic effects can be rather difficult to calculate in a rigorous way. In the present work IIS losses in photoelectron propagation were estimated semiclassically,[97] in terms of the density-dependent mean-free path (*inelastic mean free path, IMFP*[5,6,98]) of the photoelectron $\lambda(k)$, yielding energy dependent reductions. This approximation does not provide a complete description of energy-dependent IIS processes and other possible many-body effects. A more accurate theoretical description requires inclusion of different electron correlation effects in ground, final ionic and final continuum states.[19,72]

Results and discussion

Low photon-energy range (300-850 eV)

Ethyl trifluoroacetate

The photoelectron spectrum of the ESCA molecule recorded at 340 eV was thoroughly discussed in Ref.,[36] and we will only briefly review it here. The spectrum is shown in Fig.1 together with the theoretical predictions of both the anti-gauche and the anti-anti conformer.

The 1*s* photoelectron peak profiles associated with each of the carbon atoms are quite broad and reflect extensive vibrational progressions accompanying the ionization events. Moreover, a thorough theoretical analysis showed that all the bonds between second-row atoms in this molecule are weakened upon C 1*s* core ionization irrespective of which carbon is the site of ionization.[36] This is in line with very recent photoelectron-ion coincidence studies, which demonstrated rather limited atomic site-specificity in C 1*s* photofragmentation of the ESCA molecule.[99] One can argue that slightly increased yields of CF_x and F fragments at the C_{CF_3} and C_{CO} ionization sites[99] correlate with the amount of excitation of the dominant $9A'$ vibrational mode, associated with C_{CF_3}–C_{CO} and C–F stretching.[36]

Spectra similar to those in Fig. 1 were recorded for a wide range of photon energies (305 – 700 eV). The area under each C 1*s* peak is proportional to the corresponding partial cross section, and in an ideal experiment it would be possible to map out the cross section as a function of the photon energy. However during such a series of measurements the experimental conditions vary slightly over several hours (e.g. pressure, small variations in photon flux etc.). These are variations that in principle can be handled but in practice are difficult to correct to a sufficiently high degree of accuracy.

The measurement of cross sections for each of the four C 1*s* core photoelectron peaks is therefore a complex problem. For that reason, we choose the same strategy as in Ref.,[22] namely to monitor the *ratios* of the C 1*s* photoelectron intensities for each photon energy. By such a strategy we avoid the difficulties described above and can compare the experimental results to calculations.

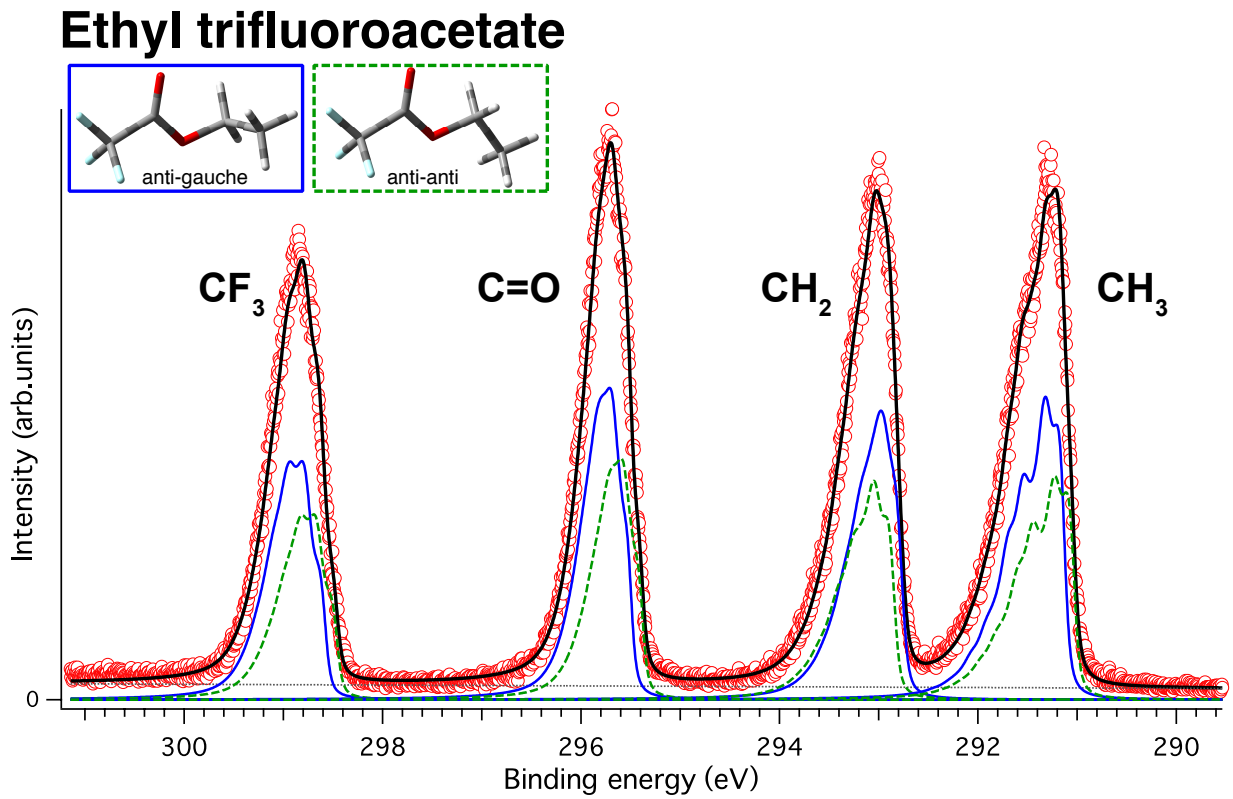

Figure 1: The high resolution C 1*s* photoelectron spectrum of the ESCA molecule (ethyl trifluoroacatate, CH_3CH_2O–(C=O)–CF_3). Blue solid and green dotted curves show Frank-Condon vibrational profiles for the *anti-gauche* and *anti-anti* conformers, respectively. The spectrum is reproduced from Ref.[36]

In the present case the ratios for the different C 1*s* photoelectron lines were obtained using the $-CH_3$ core photoelectron line as the reference, i.e. we discuss the CF_3/CH_3, C=O/CH_3 and the CH_2/CH_3 ratios.

This procedure ensures that all results are inherently normalized to gas pressure and photon flux and other long-term variations that are otherwise difficult to account for. In Fig. 2 we show the ratios obtained from the fits as well as the theoretical results discussed below.

We note that the difference in ionization energies between the C_{CH_3} and C_{CF_3} carbons is 7.5 eV, meaning that the corresponding photoelectrons have kinetic energies that differ by the same amount. This difference alone will make the C_{CF_3} cross section (lower kinetic energy) higher than the C_{CH_3} cross section by about 5% near threshold and about 3% at the highest energies of the

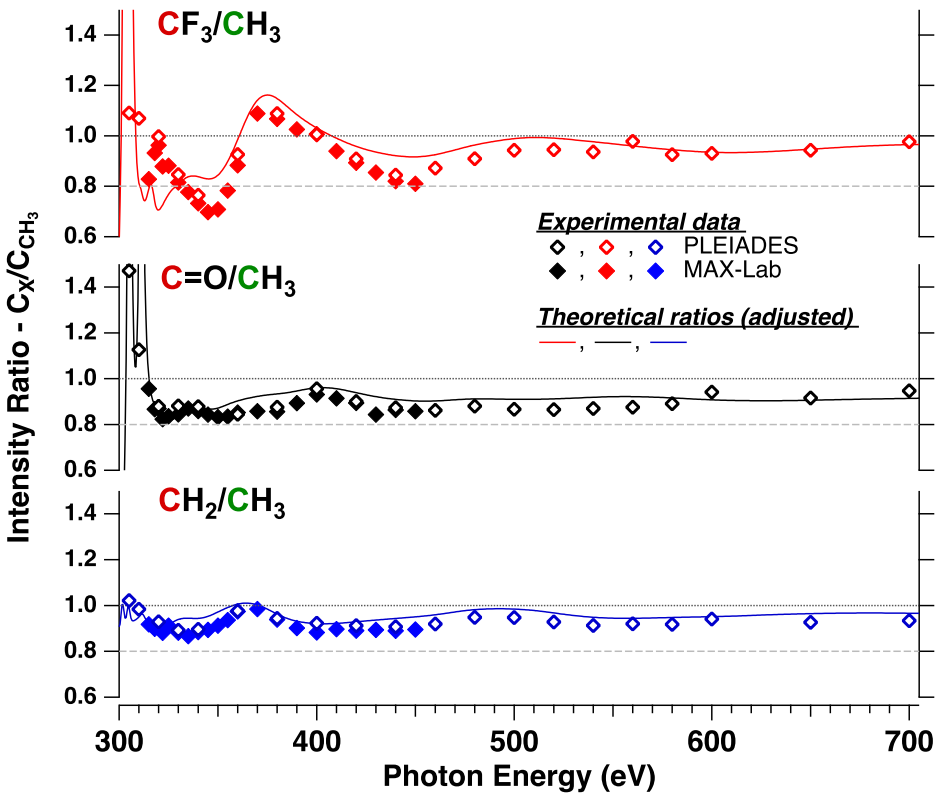

Figure 2: The relative cross section ratios for C 1*s* ionization of the three chemically different carbon atoms C_{CF_3}, $C_{C=O}$ and C_{CH_2} compared with that of the methyl carbon C_{CH_3} in ethyl trifluoroacetate. Two sets of data were obtained, one at the PLEIADES beamline at SOLEIL (open diamonds) and at the I411 beamline at MAX-lab (solid diamonds). The size of the data symbols corresponds approximately to the estimated uncertainties. The results from the two laboratories are in good agreement over almost the entire range of common photon energies. We also include the theoretical simulations based on FEFF 9 calculations (solid lines). See text for further details.

experiment. Our theoretical calculations include this effect in Fig. 2.

The efficiency of electron transmission from the ionization chamber and to detection is a complex function of kinetic energy when an advanced electron lens is used. It is difficult to measure accurately and may vary rapidly with energy near threshold.[23,100,101] This is the main reason why the results of the first 30 eV above the threshold in Fig. 2 are rather uncertain.

Fig. 2 shows that the oscillations in the relative cross sections have the largest amplitude for the C_{CF_3} carbon with the amplitudes for the other two carbons being much smaller. This can be understood since the effect is dominated by elastic scattering, similarly to EXAFS. The largest

contribution is related to the number of nearest neighboring atoms. The C_{CF_3} carbon atom is surrounded by four atoms (three fluorine and one carbon), whereas the $C_{C=O}$ and C_{CH_2} carbons are adjacent to three and two non-hydrogen atoms, respectively. A similar argument was made for the difference in scattering effect for 2-butyne where the central carbons are bonded to two closest neighbors compared to only one carbon for the terminal ones.[23]

The oscillations in relative intensities are in general smaller for the ESCA molecule than those reported for the chlorinated ethanes in Ref.[22] This can be understood by invoking the concept of scattering power – chlorine atoms are considerably stronger electron scatterers than are atoms of the 2^{nd} period in the Periodic Table of Elements.[102] Thus an important part of the oscillatory behavior is determined both by the number and the nature of the adjacent scatterers, while naturally the distance to the scatterers also plays a role.

The cross-section ratios at the end of the low-energy range in Fig. 2 seem to nearly reach the expected value of 1, being 0.98, 0.95, and 0.98 respectively, for the C_{CF_3}, $C_{C=O}$, and C_{CH_2} carbons, compared to values of 0.96, 0.88, and 0.79 found for mono-, di, and trichloroethane, respectively.[22] In Ref.[22] the departure from unity was tentatively attributed to direct shake effects, and to IIS effects. These effects are expected to be less pronounced in the case of fluorine ligands in comparison to the electron-rich chlorine ligands on account of the excited states of the fluorinated systems lying at much higher energies than do those of the corresponding chlorine-substituted molecules[103] and lower probability of multi-electron correlation satellites (see above in the "Mechanisms for intensity reduction of photoelectron lines" section). Another source of deviations of theoritical from the experimental CF_3/CH_3 and C=O/CH_3 ratios extracted for the ESCA molecule at this low energy range could be conjugate shake processes, which are not accounted for by the used theoretical approximations (see above in "Calculations"). This molecule has a double bond and hence is more susceptible to conjugate shake-ups at low kinetic/photon energies.[28,104,105]

Substituent effects on the C 1*s* photoionization cross sections

Methyl trifluoroacetate and *S*-ethyl trifluorothioacetate

Table 1: Experimental carbon 1s vertical energies (in eV) for ethyl trifluoroacetate, methyl trifluoroacetate, and *S*-ethyl trifluorothioacetate. Chemical shifts are given relative to C 1*s* of the CH_3 carbon.

Ethyl trifluoroacetate

C 1*s* peak	This work[a]		Travnikova *et al.*[b]		Smith and Thomas[c]	
CH_3	291.47	0.00	291.47	0.00	291.37	0.00
CH_2	293.14	1.67	293.19	1.72	293.07	1.70
C=O	295.79	4.32	295.80	4.33	295.72	4.35
CF_3	298.89	7.42	298.93	7.46	298.86	7.49

Methyl trifluoroacetate

C 1*s* peak	This work[a]		Smith and Thomas[d]	
CH_3	293.33	0.00	293.34	0.00
C=O	295.93	2.60	295.93	2.59
CF_3	299.00	5.67	299.03	5.69

***S*-ethyl trifluorothioacetate**

C 1*s* peak	This work[a]	
CH_3	291.19	0.00
CH_2	291.83	0.64
C=O	294.40	3.21
CF_3	298.63	7.44

[a] Estimated uncertainties 0.05 eV
[b] Ref.[36]
[c] Ref.[106] Reported uncertainties 0.03 eV
[d] Ref.[106] Reported uncertainties 0.05 eV

In addition to the ESCA molecule, two substitutionally related molecules were probed at MAX-lab. These are the methyl- and the thio analogues of ESCA, CH_3O-(C=O)-CF_3 (M-ESCA) and CH_3CH_2S–(C=O)–CF_3 (S-ESCA), respectively. In the latter molecule, the oxygen of the ethoxy group has been replaced with sulfur, to make a thioester.

Fig. 3 compares the spectra of all three molecules measured at a photon energy of 340 eV using the same experimental conditions. The spectrum of the methyl analogue at top shows well separated peaks. The effect of replacing the CH_3CH_2O- group with CH_3O- is seen to shift the spectrum slightly to higher binding energies, possibly because of the somewhat smaller polarizability of the methoxy group.[106,107]

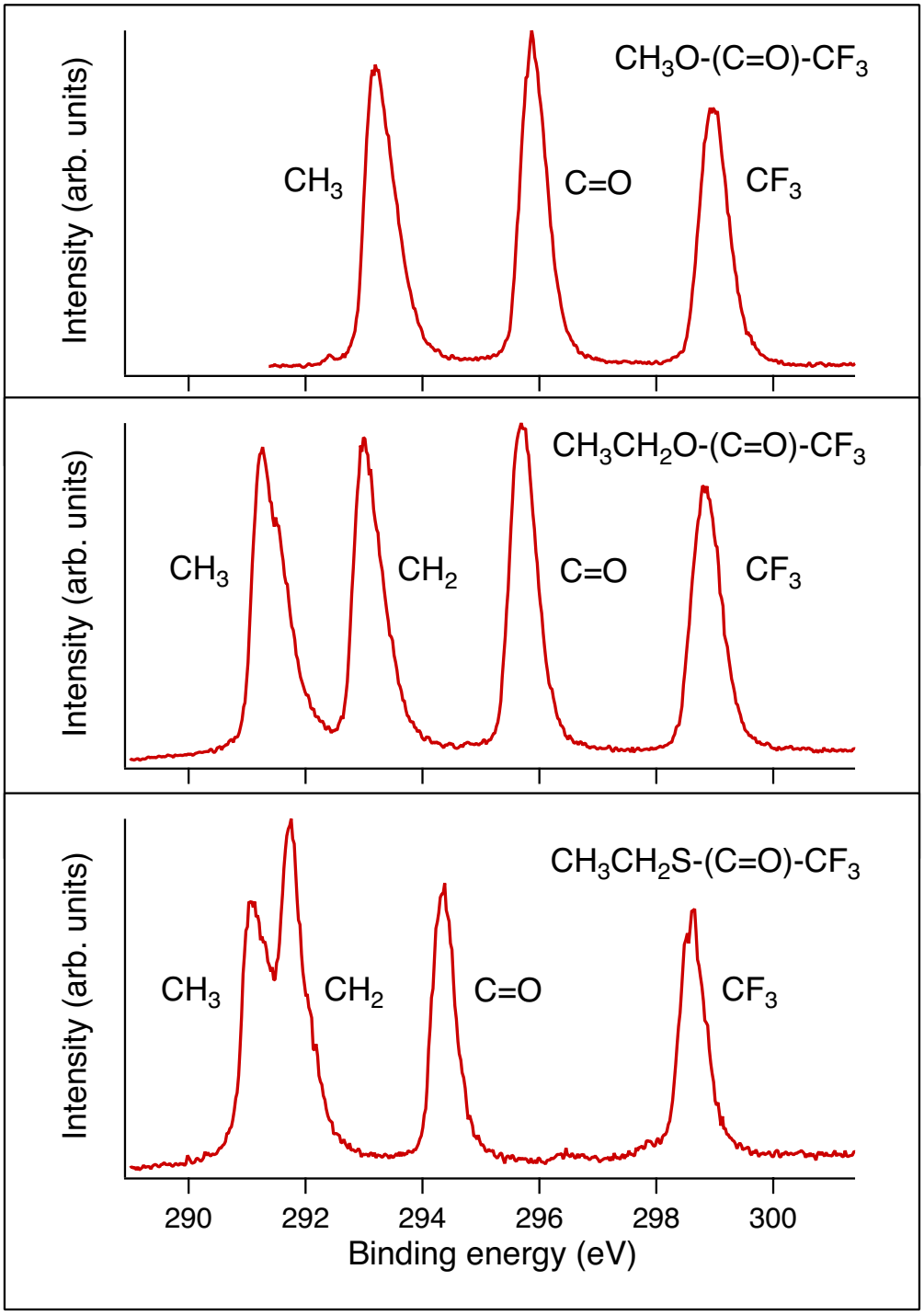

Figure 3: Carbon 1*s* photoelectron spectra of methyl trifluoroacetate (top), ethyl trifluroacetate (middle), and S-ethyl trifluorothioacetate (bottom). The spectra are recorded at a photon energy of 340 eV. All spectra were recorded at beamline I411 at the MAX II facility in Lund, Sweden.

The spectrum of the thio analogue at the bottom shows the effect of replacing oxygen in the ethoxy group with sulfur. The spectrum is now shifted towards lower binding energies due to the larger polarizability of the thioethyl group and the lower electronegativity of sulfur compared to oxygen. The largest shifts, however, are found for the closest neighbors to sulfur, i.e. the carbons of the C=O and CH_2-groups, with shifts of -1.4 and -1.3 eV, respectively. The shifts of the C_{CH_3} and C_{CF_3} carbons are both about -0.3 eV and much smaller. This leads to the overlap of the C_{CH_3} and C_{CH_2} peaks observed in the spectrum. Experimental vertical energies for the three molecules are given in Table 1. The agreement with results from previous measurements of ethyl- and methyl trifluoroacetate is excellent.

A closer look at the three spectra in Fig. 3 reveals that the linewidths are quite large. For the ESCA molecule the FWHM is about three times larger than for CO_2. This is to a minor part because the molecule in the gas phase is a mixture of two conformers,[54] each with a different set of binding energies.[36] The main reason is, however, large geometrical changes due to core ionization at each site, resulting in wide Frank-Condon envelopes that dominate the linewidths.[36]

For methyl trifluoroacetate only a single conformer has been found experimentally,[55,56] but the widths of the vibrational envelopes are nevertheless of the same magnitude as for the ESCA molecule. Separate calculations of optimized ionized states reveal that also for this molecule geometrical relaxations are large and mainly responsible for the observed broad lineshapes.

The linewidths for *S*-ethyl trifluorothioacetate, on the other hand, are smaller than for the other two compounds, despite the fact that this molecule in the gas phase exists as two conformers with similar distribution as for the ESCA molecule.[57] The narrower lines indicate smaller geometrical changes upon core ionization and may be rationalized in terms of lower atomic charges in the thioether as compared to the ESCA molecule, cf. Ref.[36]

Preparing to compare relative cross sections between the three molecules, we notice that the –(C=O)–CF_3 fragment is a common motif among the three, with differences confined to the ether/thioether functional group. The intensity ratio that is commensurable between all molecules is therefore the C=O/CF_3 ratio, which becomes our main quantity of interest. This is different

from the data presented in Fig. 2 where all intensities were computed relative to that associated with CH_3.

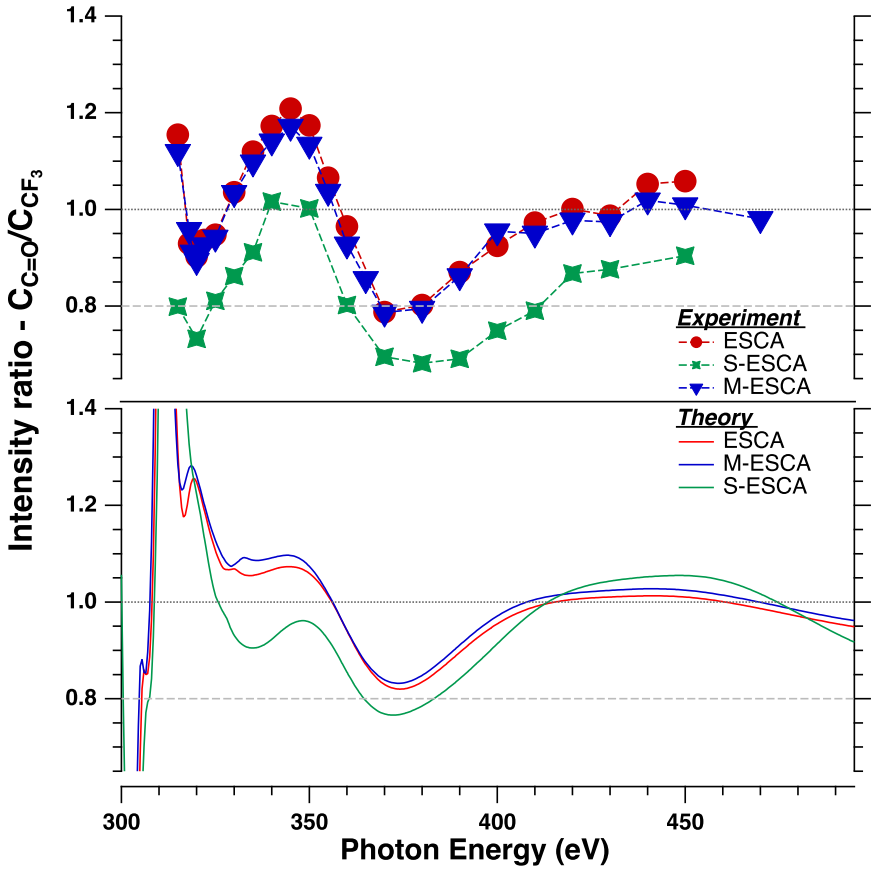

Figure 4: Experimental and calculated cross sections for carbon 1*s* ionization of the C=O carbon relative to CF_3 for ethyl trifluoroacetate (ESCA), methyl trifluoroacetate (M-ESCA), and S-ethyl trifluorothioacetate (S-ESCA). The size of the data point symbols approximately corresponds to the size of the error bars.

Fig. 4 shows the variation of the C=O/CF_3 ratio with photon energy for the three molecules. The experimental results are displayed in the upper part and may be compared with theoretical calculations shown in the lower part of the figure. As expected from Fig. 2, the overall shape of the oscillations is dominated by strong variations in the intensity of the C_{CF_3} carbon in this energy range.

Focusing first on the experimental results, one notes that both the shape and energy variation are quite similar for all molecules. For the thioester (S-ESCA), substituting sulfur for oxygen as a

nearest neighbor to the carbonyl moiety reduces the C=O/CF_3 ratio by some 17% from the values measured for the ESCA molecule. Closer scrutiny of the data shows that the CF_3/C_2H_5 intensity ratio (not included here) is very similar between ESCA and S-ESCA, implying that the observed difference in the C=O/CF_3 ratio may be ascribed to the differential effect of sulfur vs oxygen on C=O. Possible mechanisms include increased shake-up associated with the carbonyl moiety, caused by interaction with low-lying virtual orbitals on sulfur, and, acting in the same direction, inelastic scattering of photoelectrons on sulfur. However, the main reason for the reduction is found from theory, see below. Turning to a comparison between the ethoxy (ESCA) and methoxy (M-ESCA) compounds, the C=O/CF_3 cross section ratios come out equal within experimental uncertainties. Noteworthy, these two molecules differ in a next-nearest-neighboring position relative to the carbonyl moiety, one displaying a methyl group where the other molecule has a single hydrogen atom. Apparently, the intensity ratio is rather insensitive to substitution taking place two covalent bonds displaced from the site of ionization, even when the substituents in question, CH_3 and H, display quite different polarizabilities.

Theoretical estimates of the C=O/CF_3 cross section ratios are displayed in the lower part of Fig. 4. The close similarity of the graphs for ESCA and M-ESCA is well reproduced by theory. This is true also for the energy positions of the peak maxima and minima as well as the amplitudes of the oscillations, except for at low photon energies. The reduction in intensity ratio for S-ESCA as compared to ESCA and M-ESCA is essentially correctly described in the 340–380 eV range, but theory fails outside this interval. The calculations reveal that although S is a more efficient scatterer than O, this effect may be counteracted by the longer C–S bond distance compared to C–O, which are 1.76 Å[57] and 1.33 Å,[54] respectively. The bond distances are very crucial, as dephasing of scattered waves can decrease the overall scattering cross sections for certain wavelengths. In the present case this induces a reduction of the calculated XAS amplitude for $C_{C=O}$ in the 320–400 eV range compared to ESCA, in agreement with experiment. At 350 eV this relative reduction amounts to about 0.08.

In addition to effects of elastic scattering, reductions due to direct shake and IIS are verified

by the calculations. The relative reduction at 350 eV for both of these are predicted to about 0.01. Thus at this energy the main effect comes from the reduction of the XAS amplitude. However, the presently applied theory overestimates the XAS amplitude above 400 eV leading to a too pronounced maximum in the C=O/CF_3 ratio around 450 eV.

High photon-energy range (2300-6000 eV)

In previous studies of relative cross sections, the focus has been on the soft X-ray regime. Compared to the notable oscillations observed within the 100 eV above threshold (cf. Fig. 2), the C 1*s* intensity ratios level off as the photon energies approaches 1 keV and one has assumed that the high-energy asymptotic values have been reached. However, it is of practical interest to establish at which energies the cross section ratios may be regarded as converged. For this reason, we explore the energy dependence of relative cross sections for C 1*s* photoionization over a wide energy range, stretching from threshold, via the soft and tender X-ray regimes and entering the hard X-ray regime at 6 keV above threshold. In order to use the chloroethanes as a frame of reference, similar to how the soft-X-ray data was presented, Fig. 5 shows new high-energy data for intensity ratios of the chlorinated carbon to the methyl carbon (C_{CCl_x}/C_{CH_3}) for C 1*s* photoelectron lines of mono-, 1,1-di- and 1,1,1-trichloroethane. To facilitate the comparison of high- and low-energy data, previously reported low-energy data[22] on this system are also included and the photon-energy axis is drawn on a logarithmic scale. Similarly, in Fig. 6 the branching ratios for the ESCA molecule are presented up to a photon energy of 6 keV. In both Fig. 5 and Fig. 6 calculated cross-section ratios are included for comparison and shown as solid and dotted curves. The dotted curves show data as computed, whereas the solid curves are scaled to fit the high-energy experimental data.

In the high-energy region (several keV above threshold), the intensity ratios seem to have reached constant values, with no discernible oscillations. This finding is corroborated by theory, and hence we will refer to our experimental high-energy intensity ratios as the asymptotic values. However, as shown for the chloroethanes in Fig. 5, below 1 keV the ratios have not yet reached their asymptotic values. This is especially pronounced for 1,1,1-trichloroethane, but the

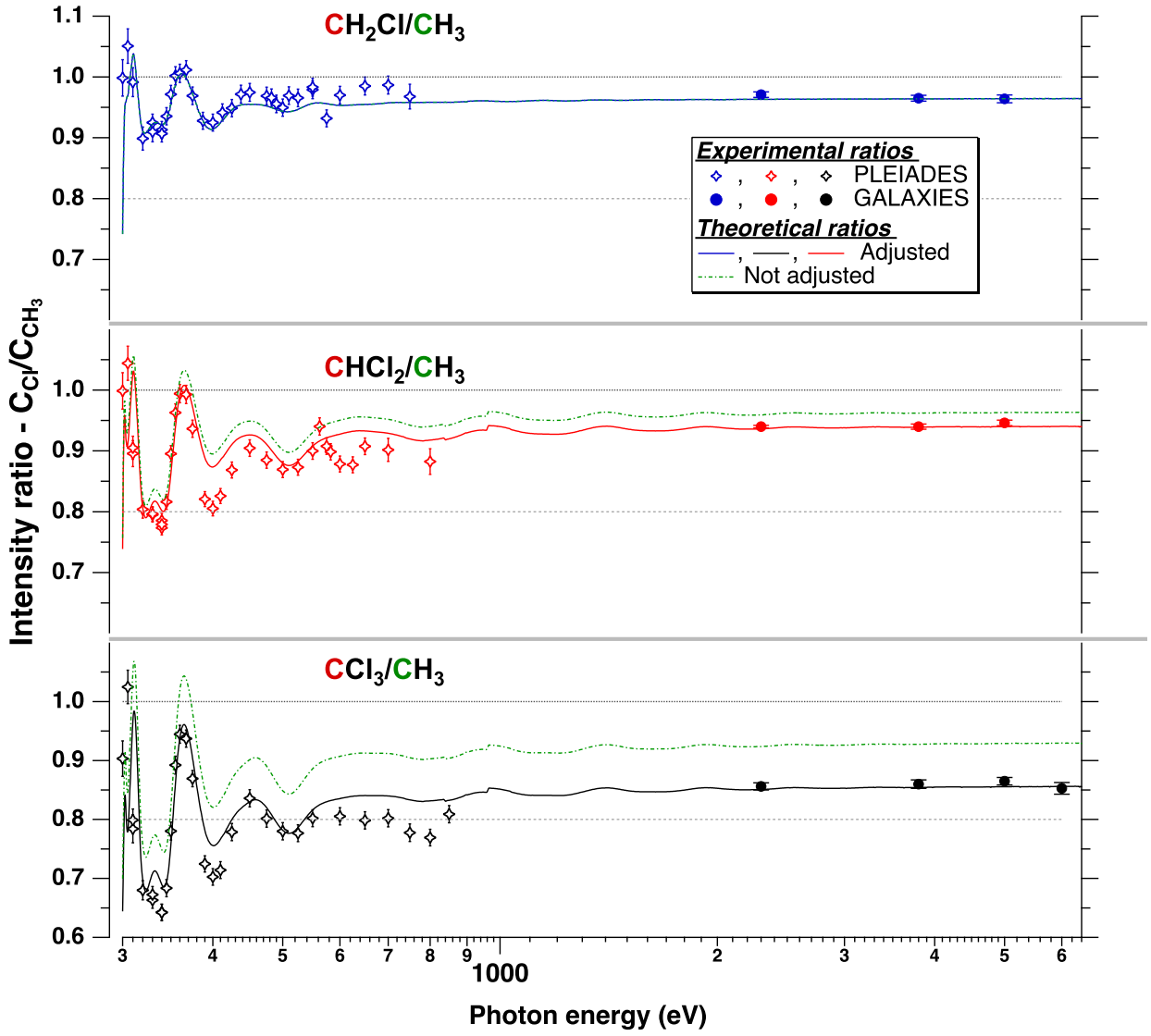

Figure 5: The relative cross section ratios up to 6 keV for C 1*s* ionization of the chemically different carbon atoms C_{CCl_x} compared with that of the methyl carbon C_{CH_3} in chloroethane (top), 1,1-dichloroethane (middle) and 1,1,1-trichloroethane (bottom). Low energy (<1 keV) data set was obtained at the PLEIADES beamline at SOLEIL [22] and high energy data (2.3–6 keV) was measured at GALAXIES beamline at SOLEIL. Calculated results are shown as solid and dotted curves, where the solid curves have been adjusted to match with the experimental high-energy data.

difference between the asymptotic values and those at the end of the low-energy region decreases with decreasing number of chlorine substituents. The deviation from the stoichiometric value of 1 follows the same trend. For the ESCA molecule, on the other hand, the differences between the values at the end of the low-energy region and the asymptotes are generally smaller than for

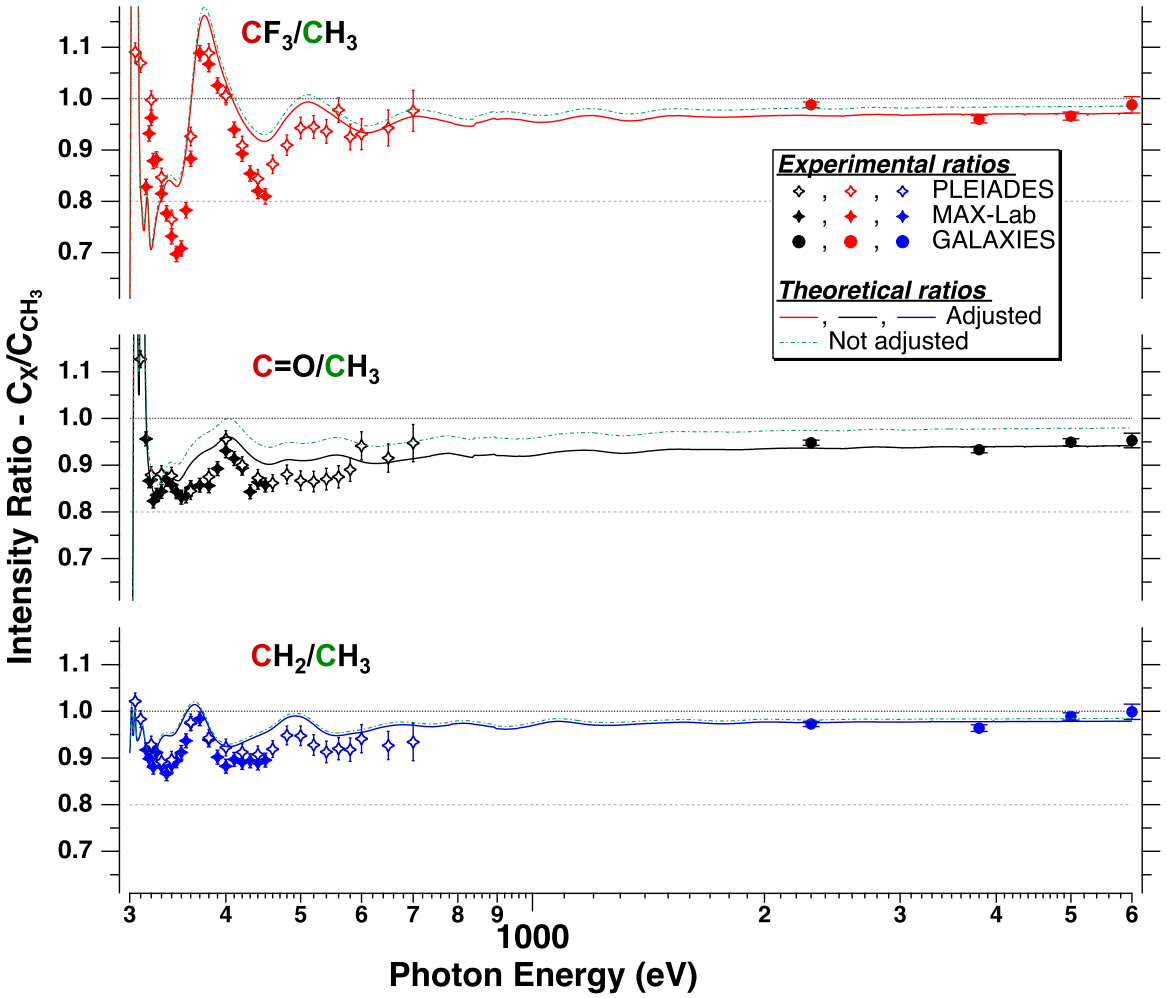

Figure 6: The relative cross section ratios up to 6 keV for C 1*s* ionization of the three chemically different carbon atoms C_{CF_3}, $C_{C=O}$ and C_{CH_2} compared with that of the methyl carbon C_{CH_3} in ethyl trifluoroacetate. Low energy (<1 keV) data set was obtained at the PLEIADES beamline at SOLEIL[22] and high energy data (2.3–6 keV) was measured at GALAXIES beamline at SOLEIL. Calculated results are shown as solid and dotted curves, where the solid curves have been adjusted to match with the experimental high-energy data.

the chloroethanes, cf. Fig. 6. The asymptotic values for the different carbon sites are also more similar to one another than observed for the chloroethanes.

For 2-butyne the C≡C/CH_3 intensity ratios was measured at two photon energies, 2.3 keV and 3.8 keV, and found to be about 0.94 in both cases. As for the ESCA molecule, this corresponds roughly to the values obtained at the end of the low-energy region.[23] Results are comparable to the high-energy values found for the C=O/CH_3 ratio in the ESCA molecule, see below.

Table 2: Experimental and calculated cross-section ratios relative to CH_3 for chloroethanes at photon energies of 600–800 eV and 2300–6000 eV. Calculated cross-section ratios of intramolecular inelastic scattering, IIS, and direct shake, DS, are included for comparison.

Ratio	$h\nu = 600-800$ eV			$h\nu = 2300-6000$ eV				Direct shakes
	Exp[a]	Calc	IIS[b]	Exp[c]	Calc	IIS[b]	DS	$CCl_xH_{(3-x)}$ / CH_3
CH_2Cl/CH_3	0.97	0.97	0.99	0.97	0.97	1.00	0.98	0.743 / 0.762
$CHCl_2/CH_3$	0.89	0.94	0.98	0.94	0.96	1.00	0.97	0.731 / 0.758
CCl_3/CH_3	0.78	0.91	0.97	0.86	0.93	0.99	0.93	0.703 / 0.754

[a] Experimental results averaged for $h\nu = 600-800$ eV to avoid possible effects of oscillations. Uncertainties are $\sim$2% estimated from the spread of the experimental data. The measurements are performed at 54.7°.
[b] Averaged calculated results.
[c] Experimental result averaged for $h\nu = 2300-6000$ eV. The uncertainties are $\sim$1% obtained purely from statistical analysis, which probably underestimates the real experimental uncertainties. The measurements are performed at 0°. The corrections for 54.7° (not included) are estimated to be within experimental uncertainties above 2 keV (see text for more details).

We will now consider the results for the high-energy asymptotes in more details. For mono-, di- and trichloroethane the ratios are about 0.97, 0.94, and 0.86, respectively (Fig. 5 and Table 2). These values reflect mainly the differences in direct shake probabilities associated with the substituted carbons and methyl carbons, which in turn is intimately connected to relaxation effects.[4,20,108] The IIS effects are energy dependent and extrinsic amplitude reduction factors should be close to unity at these energies. As the intensity ratios stay below the stoichiometric value of 1, the relaxation effects and thus the shake-up/off probabilities are higher for substituted carbon atoms compared to the methyl ones. The observed trend as a function of the degree of chlorination, is consistent with direct shake associated with the chlorines, possibly involving low-lying atomic virtual orbitals and C–Cl bonding and anti-bonding orbitals. The calculated results, presented in Table 2, confirm this assumption, but is found to underestimate the effect of direct shake both for di- and trichloroethane. The deviation increases with the number of chlorine substituents. One of the possible sources for discrepancies in prediction of direct shakes could arise from a larger multitude of the available multi-electron correlation satellite states due to strong electron correlation effects in Cl (see above).

Table 3: Experimental and calculated cross-section ratios relative CH_3 for the ESCA molecule for photon energies of 600–700 eV and 2300–6000 eV. Calculated cross-section ratios of intramolecular inelastic scattering, IIS, and direct shake, DS, are included for comparison.

Ratio	$h\nu = 600-700$ eV			$h\nu = 2300-6000$ eV				Direct shakes
	Exp[a]	Calc	IIS[b]	Exp[c]	Calc	IIS[b]	DS	CX / CH_3
CF_3/CH_3	0.98	0.96	0.97	0.98	0.98	0.99	0.99	0.755 / 0.763
C=O/CH_3	0.95	0.94	0.96	0.95	0.98	0.99	0.99	0.753 / 0.763
CH_2/CH_3	0.94	0.97	0.98	0.98	0.98	1.00	0.99	0.754 / 0.763

[a] Experimental results averaged for $h\nu = 600-700$ eV to avoid possible effects of oscillations. Uncertainties are ∼4% estimated from the spread of the experimental data. The measurements are performed at 54.7°.
[b] Averaged calculated results.
[c] Experimental result averaged for $h\nu = 2300-6000$ eV. The uncertainties are ∼1% obtained purely from statistical analysis, which probably underestimates the real experimental uncertainties. The measurements are performed at 0°. The corrections for 54.7° (not included) are estimated to be within experimental uncertainties above 2 keV (see text for more details).

The ratios of the ESCA molecule, on the other hand, show less variation with the chemical environment. For CF_3/CH_3, C=O/CH_3, and CH_2/CH_3, they are found to be about 0.98, 0.95, and 0.98, respectively (Fig. 6 and Table 3). However, it is as expected that the C=O/CH_3 ratio is likely to be more affected by shake processes since $\pi - \pi^*$ transitions are known to be responsible for strong satellite lines in core photoelectron spectra. Previous investigations of carbonyl compounds support this view.[104,105]

Also for 2-butyne one expects shake-up excitations due to $\pi - \pi^*$ transitions. This is similar to what is found for acetylene.[28,109] As noted above the asymptotic ratio for the triply bonded carbon relative to C_{CH_3} in 2-butyne is similar to the C=O/CH_3 ratio for the ESCA-molecule.

Fig. 7 shows how IIS influences the cross-section ratios for chloroethanes (a) and the ESCA molecule (b). For chloroethanes the shapes of the three curves are quite similar with minima, corresponding to maximum intensity losses, at photon energies of about 420 eV, which corresponds to the region of the most pronounced intensity oscillations. As expected from the discussion above, the intensity losses are predicted to increase with the number of chlorine atoms and to decrease with photon energy. However, losses of intensity prevail even beyond 800 eV. In Table 2 the

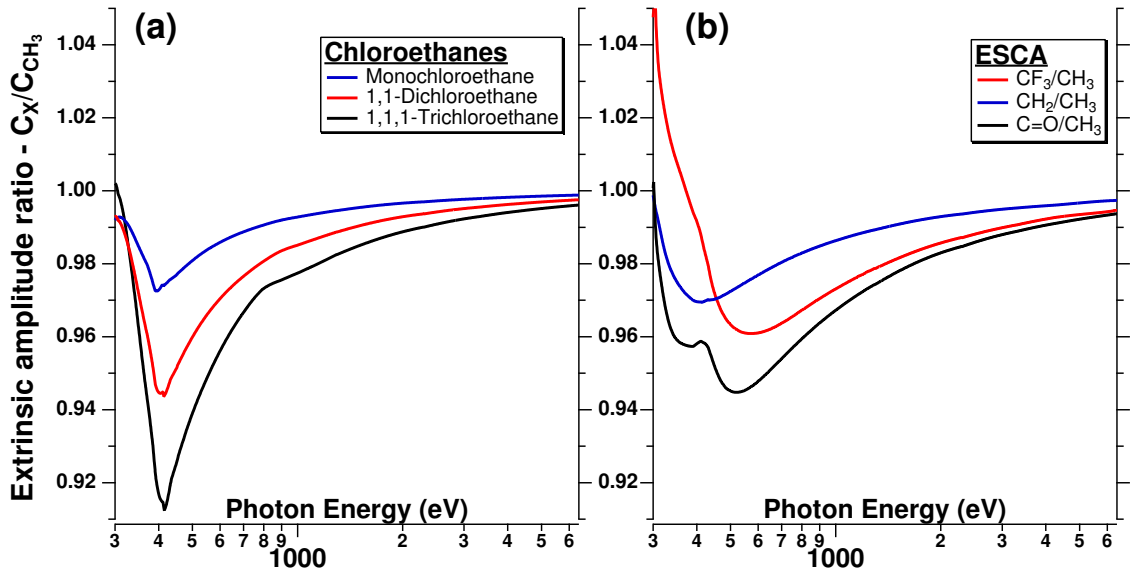

Figure 7: Calculated ratios of extrinsic reduction factors used to describe intramolecular inelastic scattering (IIS) losses in (a) chloroethanes and (b) the ESCA molecule.

difference between the experimental numbers at 600–800 eV and 2300–6000 eV represents the relative amount of IIS for each of the chlorosubstituted carbons. The differences, 0.00, 0.05, and 0.08, respectively, correspond roughly to the trend expected from the number of attached chlorine atoms, cf. Fig. 5 and 7a. The corresponding calculated numbers are smaller and again underestimate the effect of increasing number of chlorine substituents.

The extrinsic amplitude reduction factors as a function of photon energy for each of the carbon atoms in the ESCA and chloroethane molecules can be found from the supplementary material. The reduction factors are as much as 0.5–0.6 at the minimum of the curves (100–150 eV above the threshold) and converge to a common value close to 1 at high energies.

It can be seen from the Fig. 5 and Fig. 6 that the deviation at low energies between experiment and adjusted theoretical curves seems to be larger at the energies corresponding to the maximum IIS losses in chloroethanes, and are in general larger for the ESCA molecule. Thus, it can be possible that the differences in IIS caused by electron propagation through different chemical environment are underestimated by the current theory. This is an important observation, since the

IIS effects are responsible for a limited IMFP of electrons. IMFP is an essential parameter in e.g. surface science to correctly estimate the information depth of XPS signal.[5,98] Often, as was also done in the present work, IMFPs are calculated with a semi-classical jellium model which may not capture all the relative differences between the ionization sites. Our data shows that inelastic scattering varies more between different carbon sites than the calculated extrinsic reduction factors indicate, even within a single molecule.

The important result that emerges from this analysis is that a study of relative cross sections over a wide energy range makes it possible to separate the effects of IIS and direct shake processes. In addition, the analysis suggests that the discrepancy between experimental and calculated results may be due to the approximations used in the calculations at these relative high photon energies, and possibly also due to incomplete description of many-body effects.

Fig. 7b shows that the variation in IIS ratios for the ESCA molecule is quite different from those of the chloroethanes. As anticipated, the intensity losses are much less, but in addition the minima are shallower and vary with the carbon site. It is important to note that in this case we observe variations for carbon sites within one molecule. Thus, the chlorosubstituted carbon is directly bonded to the CH_3-group in the three chloroethanes, whereas only the C_{CH_2} carbon is bonded to the CH_3-group in the ESCA molecule, with the C=O and CF_3-groups being more distant.

In Table 3 experimental and calculated results are compared for the ESCA molecule. In contrast to the chloroethanes, the task of quantifying the effect of IIS is less straightforward, since the differences between ratios at 600–700 eV and 2300-6000 eV are small with relatively large uncertainties.

It can be noted that though relative cross section variations are relatively small at high energies ($<$10%, cf. Tables 2-3), the absolute losses due to shake-up and shake-off processes are considerably larger. For the chloroethanes calculations predict direct shake contributions of $\sim$24% and 26-30% for the C_{CH_3} and C_{CCl_x} 1s photoionization, respectively. The corresponding values for the ESCA molecule are $\sim$24%. These numbers are in reasonable agreement with the previous predictions of $\sim$30% for direct shake effects for carbon atoms.[110]

Similarly, the IIS effects are of comparable magnitudes at ∼425 eV, i.e. ∼130 eV above C 1*s* ionization threshold, where IIS is the strongest. For the chloroethanes the calculated IIS effects amount to 40–43% and 41–48% of the C_{CH_3} and C_{CCl_x} 1*s* photoionization, respectively, and for the ESCA molecule they are 37–40%.

This means that at any photon energy, the measured intensity of the main C 1s photoline represents 75% or less of all the C 1*s* photoionization events and at the photon energies around 100–150 eV above threshold, more than half of the total C 1*s* intensity is lost from the main peak due to inelastic scattering.

Conclusion

Relative C 1*s* cross sections for ethyl trifluoroacetate (the ESCA molecule) and related compounds, as well as in chloroethanes and 2-butyne, have been studied in the energy range from close to the threshold to 6 keV. These relative cross sections are shown to have an oscillatory behaviour in the low energy region below 1 keV due to intramolecular multiple *elastic* scattering on the neighboring atoms, in accordance with the results for chlorinated ethane molecules in Ref.[22] The relative cross sections have been modelled using FEFF 9 calculations. In the case of the ESCA molecule, these EXAFS-like oscillations have in general smaller amplitudes and also become broader with increasing excitation energy. The effect of substituting the ethoxy group CH_3CH_2O-, with CH_3CH_2S- in S-ethyl trifluoroacetate is substantial, partly due to increased direct shake and intramolecular inelastic scattering, but mainly because the effect of increased scattering amplitude of S is counteracted by the larger C–S bond length compared to C–O in ESCA. Replacing the CH_3CH_2O- group with a methoxy group, CH_3O-, shows no effect within experimental uncertainties, as expected from the small structural differences.

The observed high-energy asymptotes for C 1*s* ratios are below 1, which reflects differences of direct shake probabilities of substituted and methyl carbons. For the ESCA molecule the differences are small, but are comparable to that for the triply bonded carbon relative to C_{CH_3} in

2-butyne. The asymptotic values of chloroethanes decrease with increasing number of chlorine substituents, and the lowest asymptotic ratio of 0.86 is observed for 1,1,1-trichloroethane. This is associated with higher direct shake probabilities of carbons attached to Cl atoms.

Below 1 keV, the high energy asymptotes do not seem to be reached. The differences between the asymptotic values and those at the end of the low-energy region are probably due to intramolecular *inelastic* scattering characterised by higher cross section at lower electron kinetic energies.

We find that amplitude reduction of the main direct photoionization channel is reasonably well described by theoretical modelling, though relatively simple approximations were used to describe inelastic effects (direct shakes and IIS). Larger deviations from the experiment are observed for carbon atoms adjacent to a larger number of atoms with stronger electron scattering characteristics and for low photon energies, especially for the ESCA molecule containing the C=O double bond. This indicates that estimation of direct shakes using the "sudden" approximation and calculation of IIS effects using a semi-classical approach do not provide a complete description. On the other hand, the theoretical models used in this work do not include configuration interactions nor autoionization resonances, which have a profound effect on satellite states. Therefore, the discrepancies between experiment and theory are not surprising and can be thus understood. The observed differences in intensity ratios of the main photolines recorded at soft and hard X-ray energies show that (1) particular care should be taken for the systems with high Z-elements, which are susceptible to important intensity reductions due to multi-electron correlation shakes beyond a one-particle picture (or "sudden" approximation); (2) IMFP calculations probably underestimate IIS effects for molecular systems bearing π bonds.

The region close to the ionization threshold (up to about 150 eV) corresponds to the region of the strongest EXAFS-like oscillations. The same energy region corresponds to the most significant losses of intensity of the main photoline due to inelastic effects (shakes and IIS), which are calculated to amount up to 60% for the energies around 100–150 eV above ionization threshold. This is the origin of the extreme surface sensitivity of soft X-ray photoelectron spectroscopy, since at

these energies the IMFP does not exceed more than just a couple of monolayers.

The experimental data indicates that the IIS exists at the high end of the measured soft-X-ray energies 500–800 eV above the core-ionization threshold.

Shake-off processes, whose contribution can amount to half of the direct shakes,[77,78] "knock-out" and other inelastic scattering events can generate low energy electrons ($<$100 eV).[110] Similarly to electrons generated by interatomic Coulombic decay processes (so-called *ICD*-electrons),[111] these low-energy electrons released in biological media might induce secondary ioniziation and thus play an important role in radiation damage. Therefore, understanding secondary events concomitant with X-ray photoionization is important.

The method presented here for monitoring relative cross-sections for core-electron photoionization of gas-phase molecules over a very broad energy range extending to hard x-rays gives access to estimation of inelastic electron scattering effects within an isolated molecule and allows for their separation. The direct measurements of these effects pose serious challenges to the experiments because they lead, e.g. to modification of number of emitted electrons and/or energy sharing between interacting electrons. The observed differences in intensity ratios of main photolines recorded at soft and hard X-ray energies can serve as basis for the improvement of the existing theories describing various shake and IIS effects. This method has a great potential, especially for relatively large molecular systems, for which spectral separation of the different satellite transitions is impossible.

Acknowledgement

We would like to thank T. Darrah Thomas for his contribution to this work, stimulating discussions and participation in experiments. Data collection was performed on the PLEIADES and GALAXIES beamline at SOLEIL Synchrotron, France (Proposals No. 20100762 and 20120735). We are grateful to MAX II and SOLEIL staff for stable operation of the equipment and the storage rings during the experiments. Special thanks to the PLEIADES beamline scientist C. Nicolas and manager C. Miron and I411 beamline manager M. Tchaplyguine. This work has been supported by

the European Union Seventh Framework Programme FP7/2007-2013 under Grant Agreement No. 252781 (O.T.) and the ELISA (L.S., S.S.) and CALIPSO (L.S., K.B.) programs, by the Scientific Research Council (V.R.) in Sweden (S.S., N.M.), by the Norwegian high-performance computer consortium (NOTUR) through project number NN2506K (K.B., L.S.), by I3 program (L. S, S. S.), by the Norwegian Research Council (K. B., L. S.), by Academy of Finland (M.P.), by Knut and Alice Wallenbergs Foundation (J. S.), from U.S. Department of Energy Basic Energy Sciences Grant No. DE-FG03-97ER45623 (J. J. R., J. J. K., and F. D. V.), by Triangle de la Physique, France under Contract No. 2007-010T (S. S.) and by Agence Nationale de la Recherche, France under Contract No. ANR-18-CE30-0015 (O.T.).

Supporting Information Available

- Subtraction of the background in C 1*s* electron spectra of chloroethanes at high energies.
- Understanding the C=O/CF_3 ratio for the ESCA-family members.
- Direct shakes for the-ESCA family members.
- Absolute extrinsic amplitude reduction factors for chloroethanes and the ESCA-family members.
- Comparison of extrinsic amplitude reduction factors for ESCA and S-ESCA.
- Asymmetry parameters β for 1,1,1-trichloroethane, the ESCA molecule and 2-butyne.

This material is available free of charge via the Internet at `http://pubs.acs.org/`.

Notes and References

(1) Siegbahn, K.; Nordling, C.; Fahlman, A.; Nordberg, R.; Hamrin, K.; Hedman, J.; Johansson, G.; Bergmark, T.; Karlsson, S.-E.; Lindgren, I. et al. *ESCA, atomic, molecular and solid state structure studied by means of electron spetroscopy*; Almqvist and Wiksells, Uppsala, 1967.

(2) Siegbahn, K. Electron spectroscopy for atoms, molecules, and condensed matter. *Science* **1982**, *217*, 111–121.

(3) Gelius, U.; Allan, C.; Allison, D.; Siegbahn, H.; Siegbahn, K. The electronic structure of carbon suboxide from ESCA and AB initio calculations. *Chem. Phys. Lett.* **1971**, *11*, 224 – 228.

(4) Naves de Brito, A.; Keane, M. P.; Correia, N.; Svensson, S.; Gelius, U.; Lindberg, B. J. Experimental and theoretical XPS study of model molecules for poly(methyl methacrylate). *Surf. Interface Anal.* **1991**, *17*, 94–104.

(5) Seah, M. P.; Dench, W. A. Quantitative electron spectroscopy of surfaces: A standard data base for electron inelastic mean free paths in solids. *Surf. Interface Anal.* **1979**, *1*, 2–11.

(6) Powell, C. J.; Jablonski, A. Evaluation of calculated and measured electron inelastic mean free paths near solid surfaces. *J. Phys. Chem. Ref. Data* **1999**, *28*, 19–62.

(7) David, D.; Godet, C. Derivation of dielectric function and inelastic mean free path from photoelectron energy-loss spectra of amorphous carbon surfaces. *Appl. Surf. Sci* **2016**, *387*, 1125–1139.

(8) Jablonski, A. Modeling and parameterization of photoelectrons emitted in condensed matter by linearly polarized synchrotron radiation. *Surf. Sci.* **2018**, *667*, 121–137.

(9) Yeh, J.; Lindau, I. Atomic subshell photoionization cross sections and asymmetry parameters: $1 \pm Z \pm 103$. *At. Data Nucl. Data Tables* **1985**, *32*, 1 – 155.

(10) Mårtensson, N.; Söderstrom, J.; Svensson, S.; Travnikova, O.; Patanen, M.; Miron, C.; Sæthre, L. J.; Børve, K. J.; Thomas, T. D.; J., K. J. et al. On the relation between X-ray Photoelectron Spectroscopy and XAFS. *J. Phys. Conf. Ser.* **2013**, *430*, 012131.

(11) Woodruff, D. Adsorbate structure determination using photoelectron diffraction: Methods and applications. *Surf. Sci. Rep.* **2007**, *62*, 1–38.

(12) Rothberg, G. M.; Choudhary, K. M.; denBoer, M. L.; Williams, G. P.; Hecht, M. H.; Lindau, I. Extended X-Ray Absorption Fine Structure in Photoelectron Emission. *Phys. Rev. Lett.* **1984**, *53*, 1183–1186.

(13) Oyanagi, H.; Sakamoto, K.; Shioda, R.; Kuwahara, Y.; Haga, K. Ge overlayers on Si(001) studied by surface-extended x-ray-absorption fine structure. *Phys. Rev. B* **1995**, *52*, 5824–5829.

(14) Fadley, C. S. In *Synchrotron radiation research: advances in surface and interface science techniques*; Bachrach, R. Z., Ed.; Springer US: Boston, MA, 1992; pp 421–518.

(15) Sieger, M. T.; Miller, T.; Chiang, T.-C. Site-dependent fine structure in photoemission branching ratios. *Phys. Rev. Lett.* **1995**, *75*, 2043–2046.

(16) Patanen, M.; Benkoula, S.; Nicolas, C.; Goel, A.; Antonsson, E.; Neville, J. J.; Miron, C. Interatomic scattering in energy dependent photoelectron spectra of Ar clusters. *J. Chem. Phys.* **2015**, *143*, 124306.

(17) Winkler, M.; Børve, K. J. Attenuation of slow (10–40 eV) electrons in soft nanoparticles: Size matters in argon clusters. *Phys. Rev. E* **2018**, *97*, 012604.

(18) Martin, R. L.; Shirley, D. A. Theory of core-level photoemission correlation state spectra. *J. Chem. Phys.* **1976**, *64*, 3685–3689.

(19) Arneberg, R.; Müller, J.; Manne, R. Configuration interaction calculations of satellite structure in photoelectron spectra of H_2O. *Chem. Phys.* **1982**, *64*, 249–258.

(20) Schmidt, V. Photoionization of atoms using synchrotron radiation. *Rep. Prog. Phys.* **1992**, *55*, 1483–1659.

(21) Pauly, N.; Tougaard, S. Surface and core hole effects in X-ray photoelectron spectroscopy. *Surf. Sci.* **2010**, *604*, 1193–1196.

(22) Söderström, J.; Mårtensson, N.; Travnikova, O.; Patanen, M.; Miron, C.; Sæthre, L. J.; Børve, K. J.; Rehr, J. J.; Kas, J. J.; Vila, F. D. et al. Nonstoichiometric intensities in core photoelectron spectroscopy. *Phys. Rev. Lett.* **2012**, *108*, 193005.

(23) Carroll, T. X.; Zahl, M. G.; Børve, K. J.; Sæthre, L. J.; Decleva, P.; Ponzi, A.; Kas, J. J.; Vila, F. D.; Rehr, J. J.; Thomas, T. D. Intensity oscillations in the carbon 1 s ionization cross sections of 2-butyne. *J. Chem. Phys.* **2013**, *138*, 234310.

(24) Yang, B.; Kirz, J.; Sham, T. Oxygen K-edge absorption spectra of O_2, CO and CO_2. *Phys. Lett. A* **1985**, *110*, 301–304.

(25) Björneholm, O.; Werner, J.; Ottosson, N.; Öhrwall, G.; Ekholm, V.; Winter, B.; Unger, I.; Söderström, J. Deeper insight into depth-profiling of aqueous solutions using photoelectron spectroscopy. *J. Phys. Chem. C* **2014**, *118*, 29333–29339.

(26) Hergenhahn, U.; Kugeler, O.; Rüdel, A.; Rennie, E. E.; Bradshaw, A. M. Symmetry-selective observation of the N 1s shape resonance in N_2. *J. Phys. Chem. A* **2001**, *105*, 5704–5708.

(27) Canton, S. E.; Plésiat, E.; Bozek, J. D.; Rude, B. S.; Decleva, P.; Martín, F. Direct observation of Young's double-slit interferences in vibrationally resolved photoionization of diatomic molecules. *Proc. Nat. Acad. Sci.* **2011**, *108*, 7302–7306.

(28) Kempgens, B.; Köppel, H.; Kivimäki, A.; Neeb, M.; Cederbaum, L. S.; Bradshaw, A. M. Core level energy splitting in the C 1s photoelectron spectrum of C_2H_2. *Phys. Rev. Lett.* **1997**, *79*, 3617–3620.

(29) Thomas, T. D.; Berrah, N.; Bozek, J.; Carroll, T. X.; Hahne, J.; Karlsen, T.; Kukk, E.; Sæthre, L. J. Photon energy dependence of the $1\sigma_u/1\sigma_g$ intensity ratio in carbon 1*s* photoelectron spectroscopy of ethyne. *Phys. Rev. Lett.* **1999**, *82*, 1120–1123.

(30) Argenti, L.; Thomas, T. D.; Plésiat, E.; Liu, X.-J.; Miron, C.; Lischke, T.; Prümper, G.; Sakai, K.; Ouchi, T.; Püttner, T. et al. Double-slit experiment with a polyatomic molecule: vibrationally resolved C 1s photoelectron spectra of acetylene. *New J. Phys.* **2012**, *14*, 033012.

(31) Decleva, P.; Ponzi, A.; Santizo, I. Interference and diffraction in photoelectron spectra. *J. Electron Spectrosc. Relat. Phenom.* **2014**, *195*, 307–312.

(32) Kushawaha, R. K.; Patanen, M.; Guillemin, R.; Journel, L.; Miron, C.; Simon, M.; Piancastelli, M. N.; Skates, C.; Decleva, P. From double-slit interference to structural information in simple hydrocarbons. *Proc. Nat. Acad. Sci.* **2013**, *110*, 15201–15206.

(33) Ueda, K.; Miron, C.; Plésiat, E.; Argenti, L.; Patanen, M.; Kooser, K.; Ayuso, D.; Mondal, S.; Kimura, M.; Sakai, K. et al. Intramolecular photoelectron diffraction in the gas phase. *J. Chem. Phys.* **2013**, *139*, 124306.

(34) Ayuso, D.; Kimura, M.; Kooser, K.; Patanen, M.; Plésiat, E.; Argenti, L.; Mondal, S.; Travnikova, O.; Sakai, K.; Palacios, A. et al. Vibrationally resolved B 1s photoionization cross section of BF_3. *J. Phys. Chem. A* **2015**, *119*, 5971–5978.

(35) Patanen, M.; Kooser, K.; Argenti, L.; Ayuso, D.; Kimura, M.; Mondal, S.; Plésiat, E.; Palacios, A.; Sakai, K.; Travnikova, O. et al. Vibrationally resolved C 1s photoionization cross section of CF_4. *J. Phys. B* **2014**, *47*, 124032.

(36) Travnikova, O.; Børve, K.; Patanen, M.; Söderström, J.; Miron, C.; Sæthre, L. J.; Mårtensson, N.; Svensson, S. The ESCA molecule-Historical remarks and new results. *J. Electron Spectrosc. Relat. Phenom.* **2012**, *185*, 191–197.

(37) `http://www.synchrotron-soleil.fr/en/beamlines/pleiades`.

(38) Miron, C.; Nicolas, C.; Travnikova, O.; Morin, P.; Sun, Y.; Gel'mukhanov, F.; Kosugi, N.;

Kimberg, V. Imaging molecular potentials using ultrahigh-resolution resonant photoemission. *Nat. Phys.* **2012**, *8*, 135–138.

(39) Céolin, D.; Ablett, J. M.; Prieur, D.; Moreno, T.; Rueff, J. P.; Marchenko, T.; Journel, L.; Guillemin, R.; Pilette, B.; Marin, T. et al. Hard X-ray photoelectron spectroscopy on the GALAXIES beamline at the SOLEIL synchrotron. *J. Electron Spectrosc. Relat. Phenom.* **2013**, *190*, 188–192.

(40) Rueff, J.-P.; Ablett, J. M.; Céolin, D.; Prieur, D.; Moreno, T.; Balédent, V.; Lassalle-Kaiser, B.; Rault, J. E.; Simon, M.; Shukla, A. The GALAXIES beamline at the SOLEIL synchrotron: inelastic X-ray scattering and photoelectron spectroscopy in the hard X-ray range. *J. Synchrotron Radiat.* **2015**, *22*, 175–179.

(41) Bässler, M.; Forsell, J.; Björneholm, O.; Feifel, R.; Jurvansuu, M.; Aksela, S.; Sundin, S.; Sorensen, S.; Nyholm, R.; Ausmees, A. et al. Soft X-ray undulator beam line I411 at MAX-II for gases, liquids and solid samples. *J. Electron Spectrosc. Relat. Phenom.* **1999**, *101*, 953–957.

(42) Myrseth, V.; Bozek, J. D.; Kukk, E.; Sæthre, L. J.; Thomas, T. D. Adiabatic and vertical carbon 1s ionization energies in representative small molecules. *J. Electron Spectrosc. Relat. Phenom.* **2002**, *122*, 57–63.

(43) Kukk, E.; Snell, G.; Bozek, J. D.; Cheng, W.-T.; Berrah, N. Vibrational structure and partial rates of resonant Auger decay of the N1 $\vec{s}$ 2π core excitations in nitric oxide. *Phys. Rev. A* **2001**, *63*, 062702.

(44) Kukk, E.; Ueda, K.; Hergenhahn, U.; Liu, X.-J.; Prümper, G.; Yoshida, H.; Tamenori, Y.; Makochekanwa, C.; Tanaka, T.; Kitajima, M. et al. Violation of the Franck-Condon principle due to recoil effects in high energy molecular core-level photoionization. *Phys. Rev. Lett.* **2005**, *95*, 133001.

(45) Patanen, M.; Travnikova, O.; Zahl, M. G.; Söderström, J.; Decleva, P.; Thomas, T. D.; Svensson, S.; Mårtensson, N.; Børve, K. J.; Sæthre, L. J. et al. Laboratory-frame electron angular distributions: Probing the chemical environment through intramolecular electron scattering. *Phys. Rev. A* **2013**, *87*, 063420.

(46) Holme, A.; Saethre, L. J.; Borve, K. J.; Thomas, T. D. Chemical reactivity of alkenes and alkynes as seen from activation energies, enthalpies of protonation, and carbon 1s ionization energies. *J. Org. Chem.* **2012**, *77*, 10105–10117.

(47) Van der Straten, P.; Morgenstern, R.; Niehaus, A. Angular dependent post-collision interaction in Auger processes. *Z. Phys. D* **1988**, *8*, 35–45.

(48) Holland, D.; Parr, A.; Ederer, D.; Dehmer, J.; West, J. The angular distribution parameters of argon, krypton and xenon for use in calibration of electron spectometers. *Nucl. Instr. Meth. Phys. Res.* **1982**, *195*, 331 – 337.

(49) Di Tommaso, D.; Decleva, P. Branching ratio deviations from statistical behavior in core photoionization. *J. Chem. Phys.* **2005**, *123*, 064311.

(50) Rehr, J. J.; Albers, R. C. Theoretical approaches to x-ray absorption fine structure. *Rev. Mod. Phys.* **2000**, *72*, 621.

(51) Rehr, J. J.; Kas, J. J.; Prange, M. P.; Sorini, A. P.; Takimoto, Y.; Vila, F. Ab initio theory and calculations of X-ray spectra. *C. R. Physique* **2009**, *10*, 548–559.

(52) Vila, F. D.; Rehr, J. J.; Rossner, H. H.; Krappe, H. J. Theoretical x-ray absorption Debye-Waller factors. *Phys. Rev. B* **2007**, *76*, 014301.

(53) Frisch, M. J.; Trucks, G. W.; Schlegel, H. B.; Scuseria, G. E.; Robb, M. A.; Cheeseman, J. R.; Scalmani, G.; Barone, V.; Mennucci, B.; Petersson, G. A. et al. Gaussian 09, Revision B.01. 2009.

(54) Defonsi Lestard, M. E.; Tuttolomondo, M. E.; Wann, D. A.; Robertson, H. E.; Rankin, D. W.; Altabef, A. B. Experimental and theoretical structure and vibrational analysis of ethyl trifluoroacetate, $CF_3CO_2CH_2CH_3$. *J. Raman Spectrosc.* **2010**, *41*, 1357–1368.

(55) Defonsi Lestard, M. E.; Tuttolomondo, M. E.; Varetti, E. L.; Wann, D. A.; Robertson, H. E.; Rankin, D. W.; Ben Altabef, A. Gas-phase structure and new vibrational study of methyl trifluoroacetate ($CF_3C(O)OCH_3$). *J. Raman Spectrosc.* **2009**, *40*, 2053–2062.

(56) Kuze, N.; Ishikawa, A.; Kono, M.; Kobayashi, T.; Fuchisawa, N.; Tsuji, T.; Takeuchi, H. Molecular structure and internal rotation of CF_3 group of methyl trifluoroacetate: gas electron diffraction, microwave spectroscopy, and quantum chemical calculation studies. *J. Phys. Chem. A* **2014**, *119*, 1774–1786.

(57) Defonsi Lestard, M. E.; Tuttolomondo, M. E.; Wann, D. A.; Robertson, H. E.; Rankin, D. W.; Ben Altabef, A. A conformational and vibrational study of $CF_3COSCH_2CH_3$. *J. Chem. Phys.* **2009**, *131*, 214303.

(58) Ghosh, S. N.; Trambarulo, R.; Gordy, W. Microwave spectra and molecular structures of fluoroform, chloroform, and methyl chloroform. *J. Chem. Phys.* **1952**, *20*, 605–607.

(59) Hellwege, K. H., Hellwege, A. M., Eds. *Landolt-Bornstein: Group II: Atomic and Molecular Physics*; Springer-Verlag: Berlin, 1976; Vol. 7.

(60) Kuchitsu, K., Ed. *Structure of free polyatomic molecules - Basic data*; Springer-Verlag: Berlin, 1998.

(61) Curtiss, L. A.; Raghavachari, K.; Redfern, P. C.; Pople, J. A. Investigation of the use of B3LYP zero-point energies and geometries in the calculation of enthalpies of formation. *Chem. Phys. Lett.* **1997**, *270*, 419 – 426.

(62) Åberg, T. Multiple excitation of a many-electron system by photon and electron impact. *Ann. Acad. Sci. Fenn., Ser A IV* **1969**, 46.

(63) Kikas, A.; Osborne, S. J.; Ausmees, A.; Svensson, S.; Sairanen, O.-P.; Aksela, S. High-resolution study of the correlation satellites in photoelectron spectra of the rare gases. *J. Electron Spectrosc. Relat. Phenom.* **1996**, *77*, 241–266.

(64) Hedin, L.; Michiels, J.; Inglesfield, J. Transition from the adiabatic to the sudden limit in core-electron photoemission. *Phys. Rev. B* **1998**, *58*, 15565–15582.

(65) Nilsson, A.; Mårtensson, N.; Svensson, S.; Karlsson, L.; Nordfors, D.; Gelius, U.; ÅĔgren, H. High resolution xĂ-ray photoelectron spectroscopy study of $Cr(CO)_6$ in the gas phase. *J. Chem. Phys.* **1992**, *96*, 8770–8780.

(66) Ågren, H.; Roos, B. O.; Bagus, P. S.; Gelius, U.; Malmquist, P.; Svensson, S.; Maripuu, R.; Siegbahn, K. Multiple excitations and charge transfer in the ESCA N1s (NO_2) spectrum of paranitroaniline. A theoretical and experimental study. *J. Chem. Phys.* **1982**, *77*, 3893–3901.

(67) Wagner, C. D.; Davis, L. E.; Zeller, M. V.; Taylor, J. A.; Raymond, R. H.; Gale, L. H. Empirical atomic sensitivity factors for quantitative analysis by electron spectroscopy for chemical analysis. *Surf. Interface Anal.* **1981**, *3*, 211–225.

(68) Ungier, L.; Thomas, T. D. Resonance-enhanced shakeup in near-threshold core excitation of CO and N_2. *Phys. Rev. Lett.* **1984**, *53*, 435–438.

(69) Kempgens, B.; Kivimäki, A.; Köppe, H. M.; Neeb, M.; Bradshaw, A. M.; Feldhaus, J. One-electron versus multielectron effects in the near-threshold C 1s photoionization of acetylene. *J. Chem. Phys.* **1997**, *107*, 4219–4224.

(70) Krause, M. O.; Caldwell, C. D. Strong correlation and alignment near the Be 1*s* photoionization threshold. *Phys. Rev. Lett.* **1987**, *59*, 2736–2739.

(71) Neeb, M.; Kivimäki, A.; Kempgens, B.; Köppe, H. M.; Bradshaw, A. M.; Feldhaus, J. Conjugate shake-up-enhanced Auger transitions in N_2. *Phys. Rev. A* **1995**, *52*, 1224–1228.

(72) Martin, R. L.; Shirley, D. A. Theory of the neon 1*s* correlation-peak intensities. *Phys. Rev. A* **1976**, *13*, 1475–1483.

(73) Angonoa, G.; Schirmer, J. Theoretical K-shell photoelectron spectra of H_2CO and C_2H_2. *J. Mol. Struct. THEOCHEM* **1989**, *202*, 203 – 211.

(74) Schirmer, J.; Braunstein, M.; McKoy, V. Satellite intensities in the K-shell photoionization of CO. *Phys. Rev. A* **1991**, *44*, 5762–5772.

(75) Bandarage, G.; Lucchese, R. R. Multiconfiguration multichannel Schwinger study of the C(1s) photoionization of CO including shake-up satellites. *Phys. Rev. A* **1993**, *47*, 1989–2003.

(76) Thomas, T. D. Transition from adiabatic to sudden excitation of core electrons. *Phys. Rev. Lett.* **1984**, *52*, 417–420.

(77) Armen, G. B.; Åberg, T.; Karim, K. R.; Levin, J. C.; Crasemann, B.; Brown, G. S.; Chen, M. H.; Ice, G. E. Threshold double photoexcitation of argon with synchrotron radiation. *Phys. Rev. Lett.* **1985**, *54*, 182–185.

(78) Svensson, S.; Eriksson, B.; Mårtensson, N.; Wendin, G.; Gelius, U. Electron shake-up and correlation satellites and continuum shake-off distributions in X-Ray photoelectron spectra of the rare gas atoms. *J. Electron Spectrosc. Relat. Phenom.* **1988**, *47*, 327 – 384.

(79) Manson, S. T. Satellite lines in photoelectron spectra. *J. Electron Spectrosc. Relat. Phenom.* **1976**, *9*, 21 – 28.

(80) Sukhorukov, V.; Petrov, I.; Lagutin, B.; Ehresmann, A.; Schartner, K.-H.; Schmoranzer, H. Many-electron dynamics of atomic processes studied by photon-induced fluorescence spectroscopy. *Phys. Rep.* **2019**, *786*, 1 – 60, Many-electron dynamics of atomic processes studied by photon-induced fluorescence spectroscopy.

(81) In literature a term "correlation satellites" is sometimes used to refer to satellite states requiring consideration of multi-electron correlation effects in photoionization to distinguish them from 2-electron processes, which often can be described using simple theoretical models. However, this is misleading as all 2-electron processes – direct, conjugate and shake-off – imply electron correlation. We suggest to use "multi-electron correlation satellites" to refer to correlation satellites requiring multiple electron excitations and "2-electron correlation satellites" for photoionization processes involving only 2 electrons. It should be noted that more specific 'names' are also used to refer to correlation satellites with peculiar and particularly strong configuration mixing effects, e.g. "dynamic dipole polarization of electron shells (DPES)", "super-Coster–Kronig fluctuations", "symmetric exchange-of-symmetry (SEOS) correlations" *etc.* (see review[80] for a more detailed description of various correlation satellite effects).

(82) Svensson, S.; Karlsson, L.; Baltzer, P.; Wannberg, B.; Gelius, U.; Adam, M. Y. The photoelectron spectrum of HCl and DCl studied with ultraviolet excitation, high resolution x-ray excitation, and synchrotron radiation excitation: Isotope effects on line profiles. *J. Chem. Phys.* **1988**, *89*, 7193–7200.

(83) Svensson, S.; Eriksson, B.; Mårtensson, N.; Wendin, G.; Gelius, U. Electron shake-up and correlation satellites and continuum shake-off distributions in X-Ray photoelectron spectra of the rare gas atoms. *J. Electron Spectrosc. Relat. Phenom.* **1988**, *47*, 327–384.

(84) Carniato, S.; Selles, P.; Lablanquie, P.; Palaudoux, J.; Andric, L.; Nakano, M.; Hikosaka, Y.; Ito, K.; Marchenko, T.; Travnikova, O. et al. Photon-energy dependence of single-photon simultaneous core ionization and core excitation in CO_2. *Phys. Rev. A* **2016**, *94*, 013416.

(85) Hemmers, O.; Whitfield, S. B.; Berrah, N.; Langer, B.; Wehlitz, R.; Becker, U. Angular distributions of the C(1s) photoelectron satellites in CO. *J. Phys. B* **1995**, *28*, L693–L700.

(86) Reich, T.; Heimann, P. A.; Petersen, B. L.; Hudson, E.; Hussain, Z.; Shirley, D. A. Near-threshold behavior of the K-shell satellites in CO. *Phys. Rev. A* **1994**, *49*, 4570–4577.

(87) Goldsztejn, G.; Marchenko, T.; Püttner, R.; Journel, L.; Guillemin, R.; Carniato, S.; Selles, P.; Travnikova, O.; Céolin, D.; Lago, A. F. et al. Double-core-hole states in neon: lifetime, post-collision interaction, and spectral assignment. *Phys. Rev. Lett.* **2016**, *117*, 133001.

(88) Langer, B.; Viefhaus, J.; Hemmers, O.; Menzel, A.; Wehlitz, R.; Becker, U. High-resolution photoelectron spectrometry study of conjugate shakeup processes in the Li 1s threshold region. *Phys. Rev. A* **1991**, *43*, 1652–1655.

(89) Southworth, S.; LeBrun, T.; Azuma, Y.; Dyall, K. Argon KM photoelectron satellites. *J. Electron Spectrosc. Relat. Phenom.* **1998**, *94*, 33 – 38.

(90) Cubaynes, D.; Diehl, S.; Wuilleumier, F. J.; Meyer, M.; Heinecke, E.; Richter, T.; Zimmermann, P. Intensity inversion between main and satellite lines in atomic photoionization. *Phys. Rev. Lett.* **2007**, *99*, 213004.

(91) Fritzsche, S.; Jänkälä, K.; Huttula, M.; Urpelainen, S.; Aksela, H. Photoelectron satellite structure from the 3*d* and 4*d* inner-shell ionization of rubidium and cesium: Role of atomic relaxation. *Phys. Rev. A* **2008**, *78*, 032514.

(92) McCarthy, I.; Weigold, E. (e, 2e) spectroscopy. *Phys. Rep.* **1976**, *27*, 275–371.

(93) Schneider, T.; Chocian, P. L.; Rost, J.-M. Separation and identification of dominant mechanisms in double photoionization. *Phys. Rev. Lett.* **2002**, *89*, 073002.

(94) Koulentianos, D.; Puttner, R.; Goldsztejn, G.; Marchenko, T.; Travnikova, O.; Journel, L.; Guillemin, R.; Ceolin, D.; Piancastelli, M. N.; Simon, M. et al. KL double core hole pre-edge states of HCl. *Phys. Chem. Chem. Phys.* **2018**, *20*, 2724–2730.

(95) Nakano, M.; Penent, F.; Tashiro, M.; Grozdanov, T. P.; Žitnik, M.; Carniato, S.; Selles, P.; Andric, L.; Lablanquie, P.; Palaudoux, J. et al. Single photon K^{-2} and $K^{-1}K^{-1}$ double core ionization in $\mathbf{C}_2\mathbf{H}_{2n}$ (n=1˘3), CO, and $\mathbf{N}_2$ as a potential new tool for chemical analysis. *Phys. Rev. Lett.* **2013**, *110*, 163001.

(96) Lablanquie, P.; Grozdanov, T. P.; Žitnik, M.; Carniato, S.; Selles, P.; Andric, L.; Palaudoux, J.; Penent, F.; Iwayama, H.; Shigemasa, E. et al. Evidence of single-photon two-site core double ionization of $\mathbf{C}_2\mathbf{H}_2$ molecules. *Phys. Rev. Lett.* **2011**, *107*, 193004.

(97) Aryasetiawan, F.; Gunnarsson, O. The GW method. *Rep. Prog. Phys.* **1998**, *61*, 237–312.

(98) Tanuma, S.; Powell, C. J.; Penn, D. R. Calculations of electron inelastic mean free paths. IX. Data for 41 elemental solids over the 50 eV to 30 keV range. *Surf. Interface Anal.* **2011**, *43*, 689–713.

(99) Inhester, L.; Oostenrijk, B.; Patanen, M.; Kokkonen, E.; Southworth, S. H.; Bostedt, C.; Travnikova, O.; Marchenko, T.; Son, S.-K.; Santra, R. et al. Chemical understanding of the limited site-specificity in molecular inner-shell photofragmentation. *J. Chem. Phys. Lett.* **2018**, *9*, 1156–1163.

(100) Jauhiainen, J.; Ausmees, A.; Kivimäkia, A.; Osborne, S. J.; Naves de Briton, A.; Aksela, S.; Svensson, S.; Aksela, H. A method to determine a transmission correction for electron spectrometers using synchrotron radiation. *J. Electron Spectrosc. Relat. Phenom.* **1994**, *69*, 181–187.

(101) Niskanen, J.; Urpelainen, S.; Aksela, S.; Aksela, H.; Vahtras, O.; Carravetta, V.; Ågren, H. Valence photoionization of the LiCl monomer and dimer. *Phys. Rev. A* **2010**, *81*, 043401.

(102) Teo, B.-K.; Lee, P. A. Ab initio calculations of amplitude and phase functions for extended x-ray absorption fine structure spectroscopy. *J. Am. Chem. Soc.* **1979**, *101*, 2815–2832.

(103) Lempka, H. J.; Passmore, T. R.; Price, W. C. The photoelectron spectra and ionized states of the halogen acids. *Proc. Roy. Soc. A.* **1968**, *304*, 53–64.

(104) Guest, M. F.; Rodwell, W. R.; Darko, T.; Hillier, I. H.; Kendrick, J. Configuration interaction calculations of the satellite peaks associated with C1s ionization of carbon monoxide. *J. Chem. Phys.* **1977**, *66*, 5447–5452.

(105) Keane, M.; Lunell, S.; de Brito, A. N.; Carlsson-Göthe, M.; Svensson, S.; Wannberg, B.; Karlsson, L. Effects of relaxation and hyperconjugation on shake-up transitions in X-ray excited photoelectron spectra of some small carbonyl compounds. *J. Electron Spectrosc. Relat. Phenom.* **1991**, *56*, 313–339.

(106) Smith, S.; Thomas, T. Acidities and basicities of carboxylic acids. Correlations between core-ionization energies, proton affinities, and gas-phase acidities. *J. Am. Chem. Soc.* **1978**, *100*, 5459–5466.

(107) Hansch, C.; Leo, A.; Taft, R. A survey of Hammett substituent constants and resonance and field parameters. *Chem. Rev.* **1991**, *91*, 165–195.

(108) Nordfors, D.; Nilsson, A.; Mårtensson, N.; Svensson, S.; Gelius, U.; Ågren, H. X-ray excited photoelectron spectra of free molecules containing oxygen. *J. Electron Spectrosc. Relat. Phenom.* **1991**, *56*, 117–164.

(109) Arneberg, R.; Ågren, H.; Malmquist, P.-Å.; Svensson, S. Multiple excitations in the core photoelectron spectrum of acetylene. *Chem. Phys. Lett.* **1982**, *92*, 125 – 130.

(110) Persson, P.; Lunell, S.; Szöke, A.; Ziaja, B.; Hajdu, J. Shake-up and shake-off excitations with associated electron losses in X-ray studies of proteins. *Protein Sci.* **2001**, *10*, 2480–2484.

(111) Stumpf, V.; Gokhberg, K.; Cederbaum, L. S. The role of metal ions in X-ray-induced photochemistry. *Nat. Chem.* **2016**, *8*, 237–241.

Graphical TOC Entry

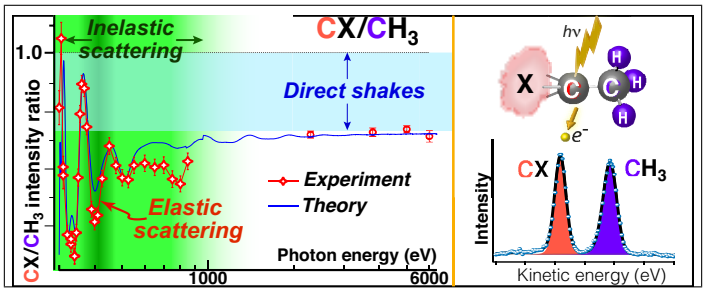

Supporting information for: Energy Dependent Relative Cross Sections in Carbon $1s$ Photoionization. Separation of Direct Shake and Inelastic Scattering Effects in Single Molecules

Oksana Travnikova,[*,†,‡] Minna Patanen,[¶] Johan Söderström,[§] Andreas Lindblad,[§] Joshua J. Kas,[‖] Fernando D. Vila,[‖] Denis Céolin,[‡] Tatiana Marchenko,[†,‡] Gildas Goldsztejn,[†] Renaud Guillemin,[†,‡] Loïc Journel,[†,‡] Thomas X. Carroll,[⊥] Knut J. Børve,[#] Piero Decleva,[@] John J. Rehr,[‖] Nils Mårtensson,[§] Marc Simon,[†,‡] Svante Svensson,[§] and Leif J. Sæthre[*,#]

LCPMR, CNRS, Sorbonne Université, UMR7614, Paris, France, Synchrotron Soleil, L'Orme des Merisiers, Saint-Aubin, F-91192 Gif-sur-Yvette Cedex, France, Nano and Molecular Systems Research Unit, Faculty of Science, 90014 University of Oulu, Finland, Department of Physics and Astronomy, Uppsala University, P.O. Box 516, 75120 Uppsala, Sweden, Department of Physics, Box 351560, University of Washington, Seattle, Washington 98195-1560, USA, Division of Natural Sciences, Keuka College, Keuka Park, New York 14478, USA, Department of Chemistry, University of Bergen, Allégaten 41, NO-5007 Bergen, Norway, and Dipartimento di Scienze Chimiche e Farmaceutiche, Universitá di Trieste and IOM-CNR, 34127 Trieste, Italy

E-mail: Oksana.Travnikova@upmc.fr; Leif.Saethre@uib.no

Contents

*To whom correspondence should be addressed

†LCPMR, CNRS, Sorbonne Université, UMR7614, Paris, France

‡Synchrotron Soleil, L'Orme des Merisiers, Saint-Aubin, F-91192 Gif-sur-Yvette Cedex, France

¶Nano and Molecular Systems Research Unit, Faculty of Science, 90014 University of Oulu, Finland

§Department of Physics and Astronomy, Uppsala University, P.O. Box 516, 75120 Uppsala, Sweden

‖Department of Physics, Box 351560, University of Washington, Seattle, Washington 98195-1560, USA

⊥Division of Natural Sciences, Keuka College, Keuka Park, New York 14478, USA

#Department of Chemistry, University of Bergen, Allégaten 41, NO-5007 Bergen, Norway

@Dipartimento di Scienze Chimiche e Farmaceutiche, Universitá di Trieste and IOM-CNR, 34127 Trieste, Italy

1 Subtraction of the background in C 1s electron spectra of chloroethanes at high energies (hν >2keV)

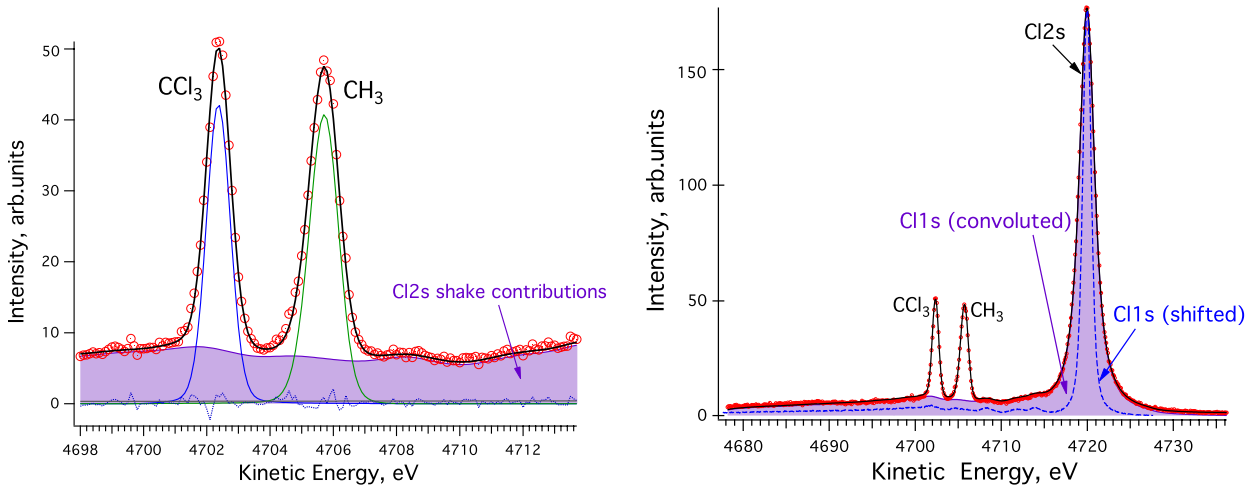

(a) C 1s photoelectron lines

(b) C 1s and Cl 2s photoelectron lines

Figure S1: Carbon 1s photoelectron spectra of tri(1,1,1)-chlroethane recorded at a photon energy of 5000 eV: (a) zoom on kinetic energy range of C 1s photoelectron lines and (b) larger kinetic energy range, showing contributions from Cl 2s photoionization. Red circles represent experimental data, black curve – fit to the experimental data, using C_{CCl_3} and C_{CH_3} C 1s contributions (thin blue and green lines, respectively) and Cl 2s shake-up contributions (purple filled curve). Cl 2s photoelectron line and corresponding shake-up contributions were modeled using Cl 1s photoelectron line (shown as dashed blue line in panel (b)) recorded at the same energy and shifted by 2551.6 eV. Dotted blue curve in (a) is a residue of the fit.

In the case of the chloroethanes we observed a strong background from Cl 2s shake contributions. Subtraction of this was made using a model taken from a Cl 1s shake spectrum.

For high-energy measurements in the case of the chloroethanes, C 1s photoelectron lines are embedded on the background from Cl 2s shake contributions. Subtraction of this was made using a model taken from a Cl 1s shake spectrum. In order to do this Cl 1s photoelectron spectra were recorded at the same time as the C 1s ones. The Cl 1s photoelectron spectrum was than shifted by about 2550 eV to match Cl 2s photoelectron lines and fitted using additional Lorenzian and Gaussian contributions to account for differences in Cl 2s/1s lifetimes and differences in Doppler broadenings due to different kinetic energies of Cl 2s/1s

photoelectrons. The profiles of the convoluted Cl 1s spectra presented a very good description of the background in C 1s photoionization spectra of chloroethanes. Theoretical profiles were used to fit $C_{CH_xCl_{3-x}}$ and C_{CH_3} C 1s photoelectron lines of chloroethanes. One example of this procedure is shown in Fig. S1 for trichloroethane recorded at 5000 eV.

2 Understanding the C=O/CF_3 ratio for the ESCA-family members.

Central to the results presented in Figure 4 is the understanding of the magnitude of the various effects, and how they determine the ratios as a function of photon energy. Part of this information is available from theoretical calculations. The theoretical curves are produced as products of three contributions: the XAS oscillation, the energy-dependent intramolecular inelastic scattering (IIS), and the energy-independent direct shake (DS). IIS was calculated as extrinsic amplitude reduction factors using a semi-classical expression for the electron propagator, and a local density approximation for the inelastic mean free path (IMFP). DS processes are estimated from S_0^2, the square of the overlap integral between the initial state wave function and the relaxed final-state wavefunction with the active core electron annihilated. Figure S2 compares the effect of XAS and IIS for S-ESCA and ESCA. It is seen that below 400 eV the ratio of XAS for S-ESCA is considerably smaller than for the ESCA molecule. This is reversed for the 400–500 eV range. The reduction effect of IIS is clearly larger for S-ESCA than ESCA, making the products of the two effects more similar to each other. The third contribution to the spectrum, the DS factor, may be found from Table S1. The absolute values for CF_3 and C=O are both smaller for S-ESCA than for ESCA. In addition the C=O/CF_3 ratio is smaller, reducing the difference between the two curves somewhat more.

Figure S2 shows that theory overestimate the XAS component of the C=O/CF_3 ratio between 400–500 eV. To understand this in more detail, Figure S3 compares the XAS ampli-

tudes of CF_3 and C=O for S-ESCA and ESCA. It is interesting to note that while the CF_3 amplitudes are almost unchanged, the variation is more pronounced for C=O, particularly below 500 eV. This is consistent with the experimental results showing that the difference in the C=O/CF_3 ratio between S-ESCA and ESCA is due to the different effect of sulfur compared to oxygen on the C=O amplitude.

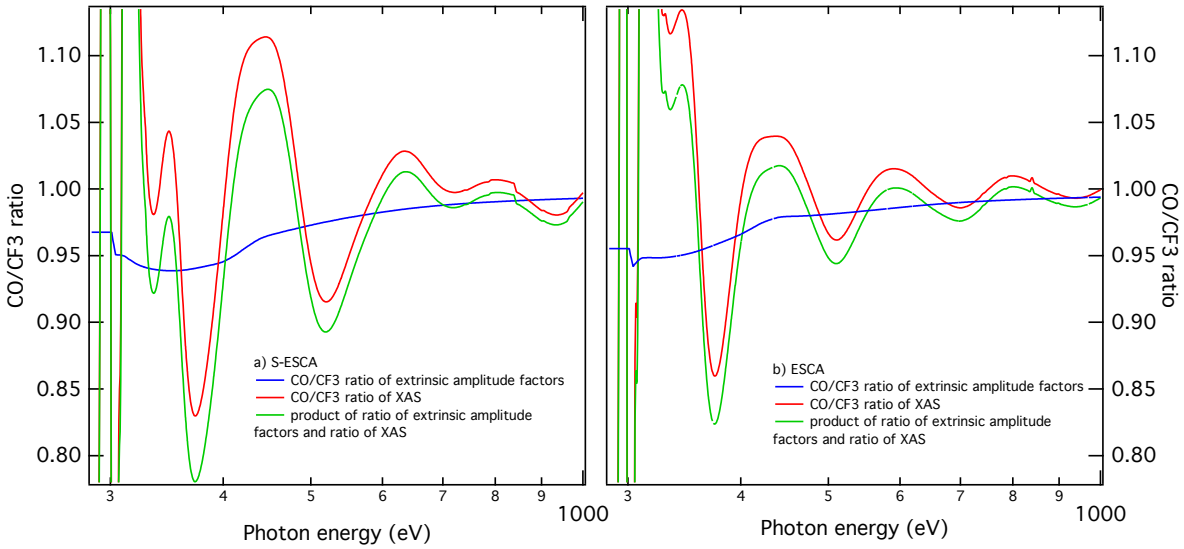

Figure S2: The ratios of C 1s cross sections of $C_{C=O}$ and C_{CF_3} carbon sites, *i.e.* XAS amplitudes, (red curves); the ratios of the corresponding extrinsic amplitude reduction factors (blue curves) and their product (green curves) for (a) S-ethyl trifluoroacetate (S-ESCA) and (b) ethyl trifluorothioacetate (ESCA).

3 Direct shakes for the ESCA-family members

Table S1: Calculated direct shakes (DS) and their ratios relative to CF_3 (CX/CF_3) for ethyl trifluoroacetate (ESCA), methyl trifluoroacetate (M-ESCA). and S-ethyl trifluorothioacetate (S-ESCA).

Carbon	ESCA		M-ESCA		S-ESCA	
	DS[a]	CX/CF_3	DS	CX/CF_3	DS[a]	CX/CF_3
CF_3	0.755	1	0.758	1	0.741	1
C=O	0.753	0.997	0.755	0.996	0.727	0.981
CH_2	0.754	0.999	–	-	0.732	0.988
CH_3	0.763	1.011	0.757	0.999	0.755	1.019

[a] Average of *anti-gauche* and *anti-anti* conformers.

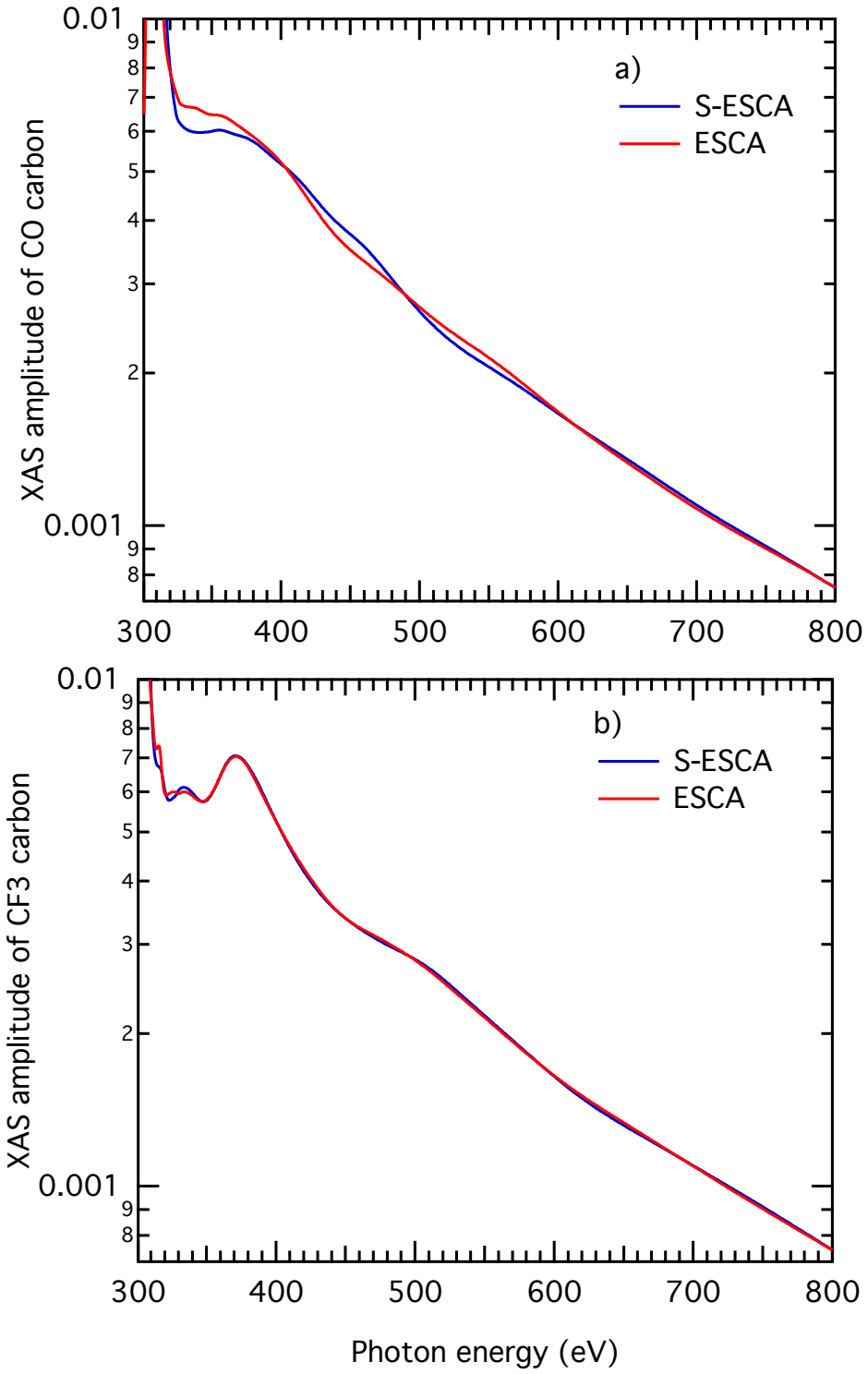

Figure S3: The cross sections, *i.e.* XAS amplitudes, of the (a) $C_{C=O}$ and (b) C_{CF_3} 1s states in ethyl trifluoroacetate, ESCA (red) and S-ethyl trifluorothioacetate, S-ESCA (blue).

4 Comparison of extrinsic amplitude reduction factors for ESCA and S-ESCA

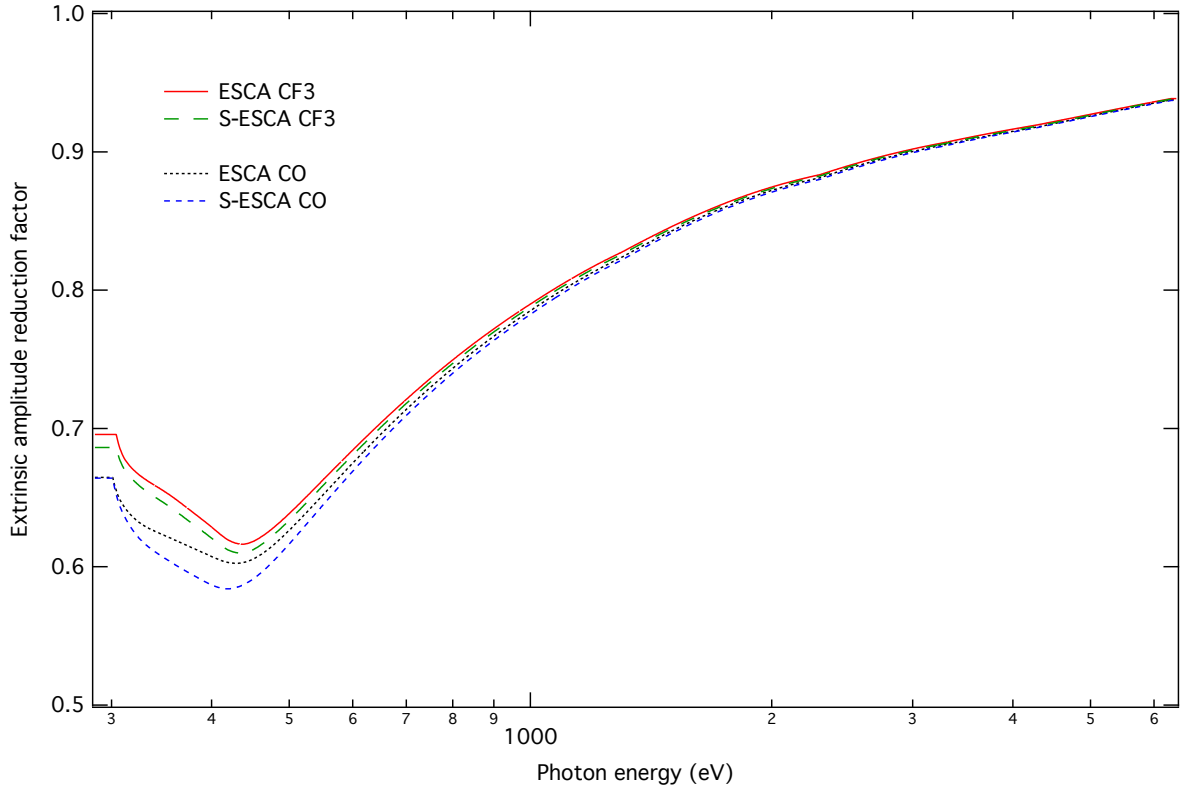

Figure S4: Comparison of calculated extrinsic amplitude reduction factors for C 1s cross sections of C_{CF_3} and $C_{C=O}$ atoms in ethyl trifluoroacetate (ESCA) and S-ethyl trifluorothioacetate (S-ESCA).

5 Absolute extrinsic amplitude reduction factors

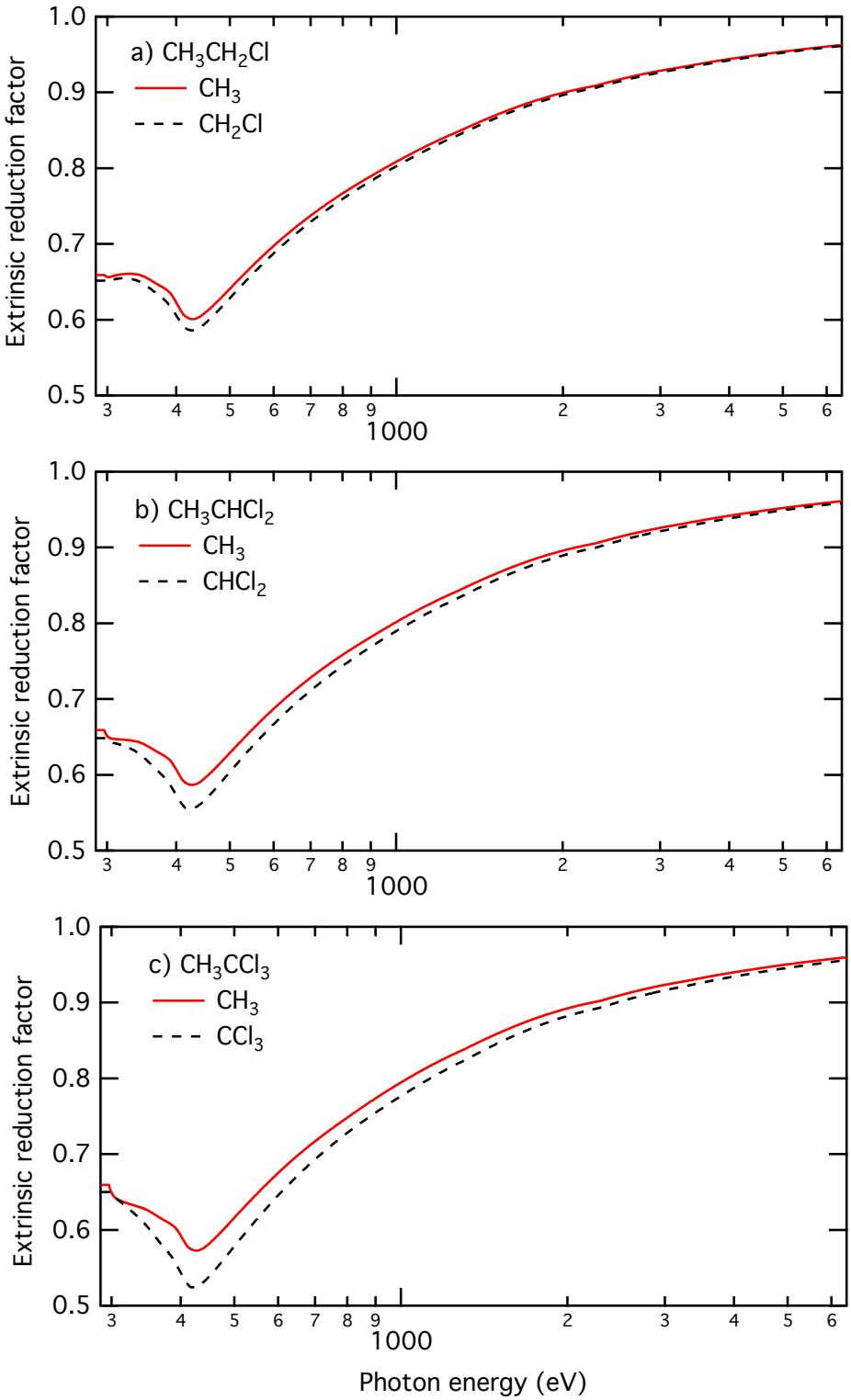

Figure S5: Calculated extrinsic amplitude reduction factors for chloroethanes: (a) monochloroethane, (b) 1,1-dichloroethane and (c) 1,1,1-trichloroethane.

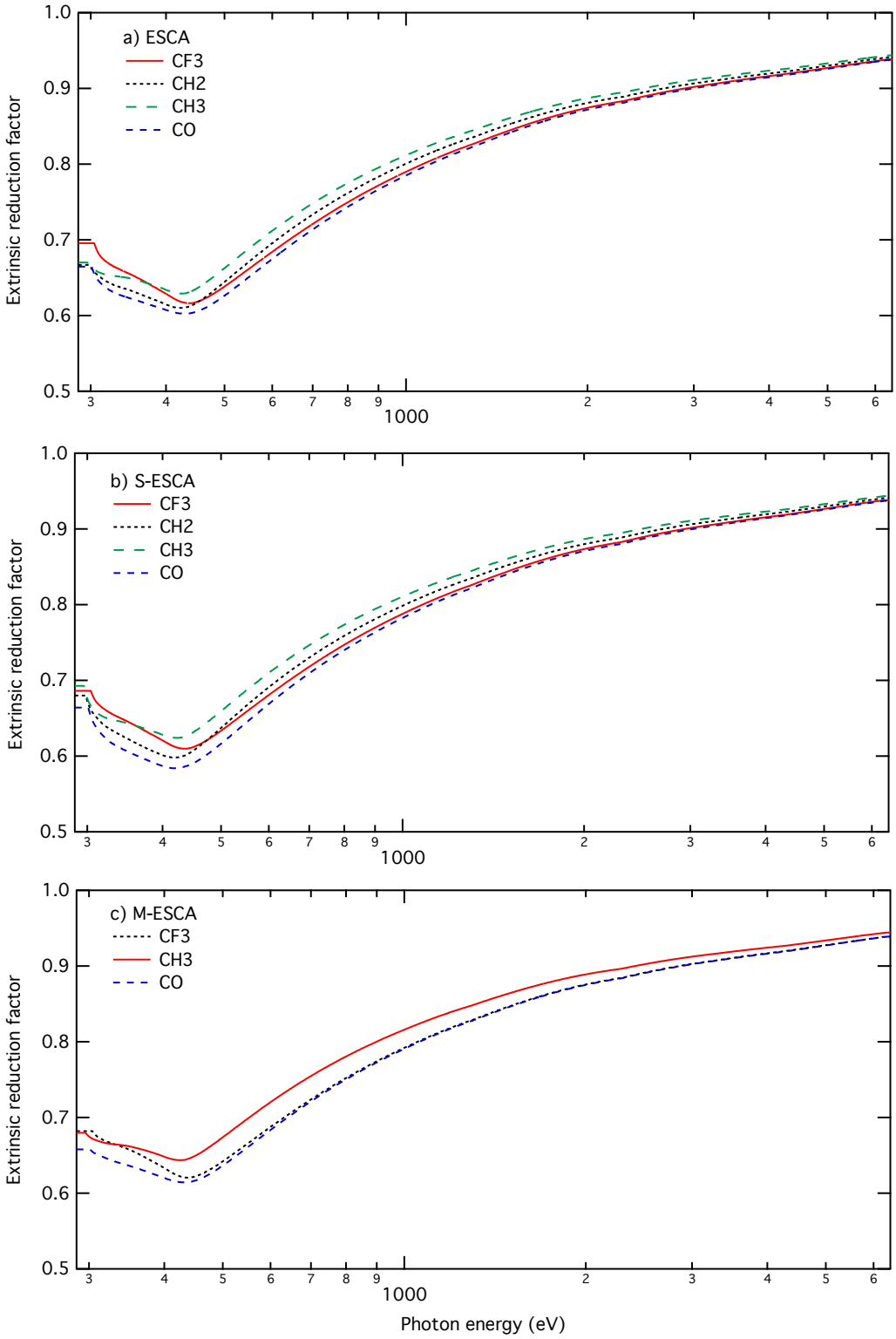

Figure S6: Calculated extrinsic amplitude reduction factors for the ESCA-family members: (a) ethyl trifluoroacetate (ESCA), (b) S-ethyl trifluorothioacetate (S-ESCA) and (c) methyl trifluoroacetate (M-ESCA).

6 Calculated asymmetry parameters β

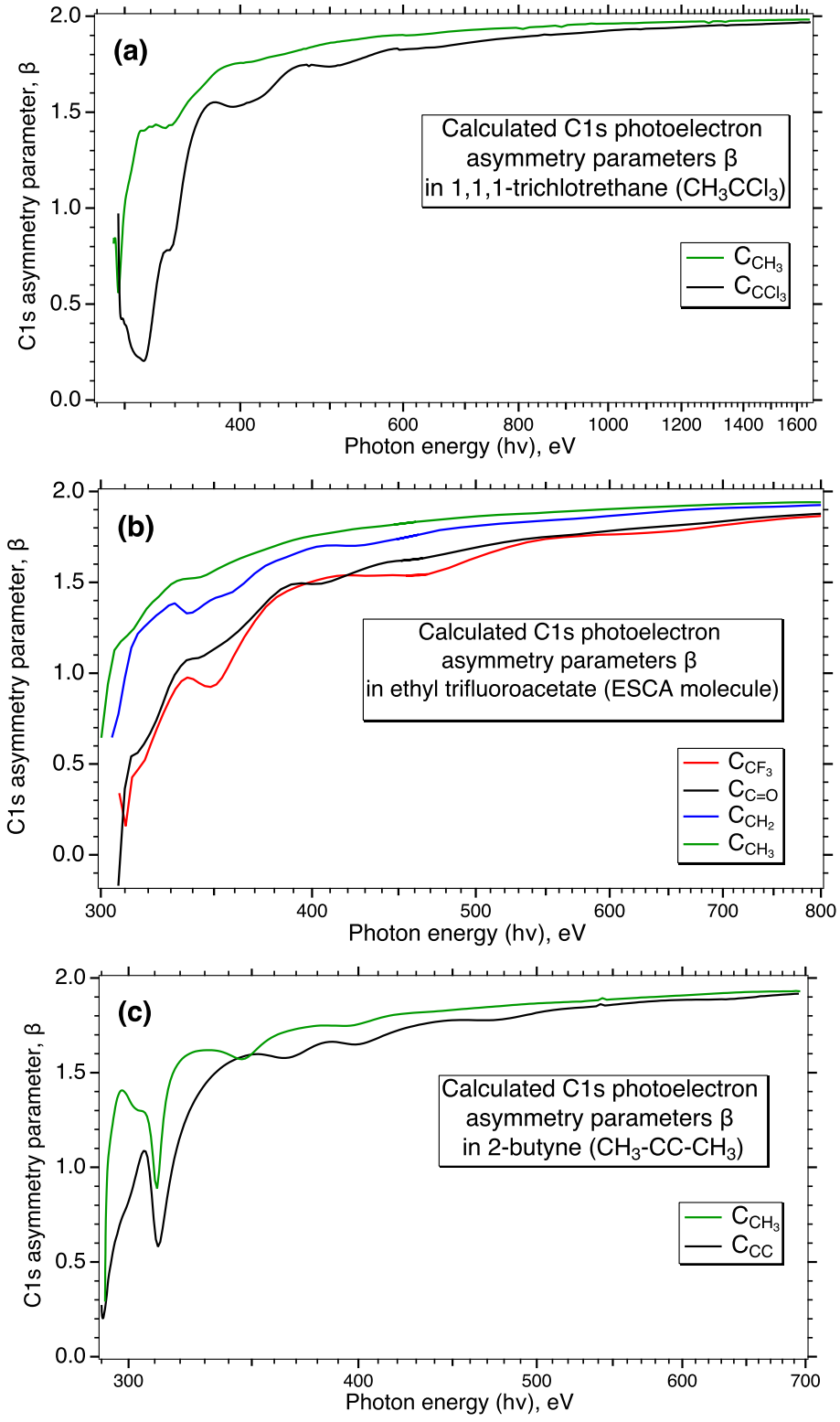

Figure S7: Calculated asymmetry parameters β for (a) 1,1,1-trichloroethane, (b) ethyl trifluoroacetate (ESCA) and (c) 2-butyne.